

1 **A HIGH ORDER ACCURATE BOUND-PRESERVING COMPACT**
2 **FINITE DIFFERENCE SCHEME FOR TWO-DIMENSIONAL**
3 **INCOMPRESSIBLE FLOW**

4 HAO LI AND XIANGXIONG ZHANG *

5 **Abstract.** For solving two-dimensional incompressible flow in the vorticity form by the fourth-
6 order compact finite difference scheme and explicit strong stability preserving (SSP) temporal dis-
7 cretizations, we show that the simple bound-preserving limiter in [5] can enforce the strict bounds
8 of the vorticity, if the velocity field satisfies a discrete divergence free constraint. For reducing
9 oscillations, a modified TVB limiter adapted from [2] is constructed without affecting the bound-
10 preserving property. This bound-preserving finite difference method can be used for any passive
11 convection equation with a divergence free velocity field.

12 **Key words.** Finite difference, monotonicity, bound-preserving, discrete maximum principle,
13 passive convection, incompressible flow, total variation bounded limiter.

14 **AMS subject classifications.** 65M06, 65M12

15 **1. Introduction.** In this paper, we are interested in constructing high order
16 compact finite difference schemes solving the following two-dimensional time-dependent
17 incompressible Euler equation in vorticity and stream-function formulation

18 (1.1a) $\omega_t + (u\omega)_x + (v\omega)_y = 0,$

19 (1.1b) $\psi = \Delta\omega,$

20 (1.1c) $\langle u, v \rangle = \langle -\psi_y, \psi_x \rangle,$

21 with periodic boundary conditions and suitable initial conditions. In the above for-
22 mulation, ω is the vorticity, ψ is the stream function, $\langle u, v \rangle$ is the velocity and Re
23 is the Reynolds number.

24 For simplicity, we only focus on the incompressible Euler equation (1.1). With
25 explicit time discretizations, the extension of high order accurate bound-preserving
26 compact finite difference scheme to Navier-Stokes equation

27 (1.2) $\omega_t + (u\omega)_x + (v\omega)_y = \frac{1}{Re}\Delta\omega$

28 would be straightforward following the approach in [5].

29 The equation (1.1c) implies the incompressibility condition

30 (1.3) $u_x + v_y = 0.$

31 Due to (1.3), (1.1a) is equivalent to

32 (1.4) $\omega_t + u\omega_x + v\omega_y = 0$

33 for which the initial value problem satisfies a bound-preserving property:

34
$$\min_{x,y} \omega(x, y, 0) = m \leq \omega(x, y, t) \leq M = \max_{x,y} \omega(x, y, 0).$$

*Department of Mathematics, Purdue University, 150 N. University Street, West Lafayette,
IN 47907-2067 (li2497@purdue.edu, zhan1966@purdue.edu). Research is supported by NSF DMS-
1913120.

35 If solving (1.4) directly, it is usually easier to construct a bound-preserving scheme.
 36 For the sake of conservation, it is desired to solve the conservative form equation
 37 (1.1a). The divergence free constraint (1.3) is one of the main difficulties in solving
 38 incompressible flows. In order to enforce the bound-preserving property for (1.1a)
 39 without losing accuracy, the incompressibility condition must be properly used since
 40 the bound-preserving property may not hold for (1.1a) without (1.3), see [9, 8, 10].

41 Even though the bound-preserving property and the global conservation imply
 42 certain nonlinear stability, in practice a bound-preserving high order accurate compact
 43 finite difference scheme can still produce excessive oscillations for a pure convection
 44 problem. Thus an additional limiter for reducing oscillations is often needed, e.g., the
 45 total variation bounded (TVB) limiter discussed in [2]. One of the main focuses of
 46 this paper is to design suitable TVB type limiters, without losing bound-preserving
 47 property. Notice that the TVB limiter for a compact finite difference scheme is de-
 48 signed in a quite different way from those for discontinuous Galerkin method, thus it
 49 is nontrivial to have a bound-preserving TVB limiter for the compact finite difference
 50 schemes.

51 The paper is organized as follows. Section 2 is a review of the compact finite dif-
 52 ference method and a simple bound-preserving limiter for scalar convection-diffusion
 53 equations. In Section 3, we show that the compact finite difference scheme can be
 54 rendered bound-preserving if the velocity field satisfies a discrete divergence free con-
 55 dition. We discuss the bound-preserving property of a TVB limiter in Section 4.
 56 Numerical tests are shown in Section 5. Concluding remarks are given in Section 6.

57 **2. Review of compact finite difference method.** In this section we review
 58 the compact finite difference method and a bound-preserving limiter in [5].

59 **2.1. A fourth-order accurate compact finite difference scheme.** Consider
 60 a smooth function $f(x)$ on the interval $[0, 1]$. Let $x_i = \frac{i}{N}$ ($i = 1, \dots, N$) be the
 61 uniform grid points on the interval $[0, 1]$. A fourth-order accurate compact finite
 62 difference approximation to derivatives on the interval $[0, 1]$ is given as:

$$63 \quad (2.1) \quad \begin{aligned} \frac{1}{6}(f'_{i+1} + 4f'_i + f'_{i-1}) &= \frac{f_{i+1} - f_{i-1}}{2\Delta x} + \mathcal{O}(\Delta x^4), \\ \frac{1}{12}(f''_{i+1} + 4f''_i + f''_{i-1}) &= \frac{f_{i+1} - 2f_{i-1} + f_{i-2}}{\Delta x^2} + \mathcal{O}(\Delta x^4), \end{aligned}$$

64 where f_i , f'_i and f''_i are point values of a function $f(x)$, its derivative $f'(x)$ and its
 65 second order derivative $f''(x)$ at uniform grid points x_i ($i = 1, \dots, N$) respectively.

66 Let \mathbf{f} be a column vector with numbers f_1, f_2, \dots, f_N as entries. Let W_1, W_2, D_x
 67 and D_{xx} denote four linear operators as follows:

$$68 \quad (2.2) \quad W_1 \mathbf{f} = \frac{1}{6} \begin{pmatrix} 4 & 1 & & & 1 \\ 1 & 4 & 1 & & \\ & & \ddots & \ddots & \ddots \\ & & & 1 & 4 & 1 \\ 1 & & & & 1 & 4 \end{pmatrix} \begin{pmatrix} f_1 \\ f_2 \\ \vdots \\ f_{N-1} \\ f_N \end{pmatrix}, D_x \mathbf{f} = \frac{1}{2} \begin{pmatrix} 0 & 1 & & & -1 \\ -1 & 0 & 1 & & \\ & & \ddots & \ddots & \ddots \\ & & & -1 & 0 & 1 \\ 1 & & & & -1 & 0 \end{pmatrix} \begin{pmatrix} f_1 \\ f_2 \\ \vdots \\ f_{N-1} \\ f_N \end{pmatrix},$$

69

(2.3)

$$W_2 \mathbf{f} = \frac{1}{12} \begin{pmatrix} 10 & 1 & & & 1 \\ 1 & 10 & 1 & & \\ & & \ddots & \ddots & \ddots \\ & & & 1 & 10 & 1 \\ 1 & & & & 1 & 10 \end{pmatrix} \begin{pmatrix} f_1 \\ f_2 \\ \vdots \\ f_{N-1} \\ f_N \end{pmatrix}, D_{xx} \mathbf{f} = \begin{pmatrix} -2 & 1 & & & 1 \\ 1 & -2 & 1 & & \\ & & \ddots & \ddots & \ddots \\ & & & 1 & -2 & 1 \\ 1 & & & & 1 & -2 \end{pmatrix} \begin{pmatrix} f_1 \\ f_2 \\ \vdots \\ f_{N-1} \\ f_N \end{pmatrix}.$$

71 If $f(x)$ is periodic with with period 1, the fourth-order compact finite difference
 72 approximation (2.1) to the first order derivative and second order derivative can be
 73 denoted as

$$74 \quad W_1 \mathbf{f}' = \frac{1}{\Delta x} D_x \mathbf{f}, \quad W_2 \mathbf{f}'' = \frac{1}{\Delta x^2} D_{xx} \mathbf{f},$$

75 which can be explicitly written as

$$77 \quad \mathbf{f}' = \frac{1}{\Delta x} W_1^{-1} D_x \mathbf{f}, \quad \mathbf{f}'' = \frac{1}{\Delta x^2} W_2^{-1} D_{xx} \mathbf{f},$$

78 where W_1^{-1} and W_2^{-1} are the inverse operators. For convenience, by abusing notations
 79 we let $W_1^{-1} f_i$ denote the i -th entry of the vector $W_1^{-1} \mathbf{f}$.

81 **2.2. High order time discretizations.** For time discretizations, we use the
 82 strong stability preserving (SSP) Runge-Kutta and multistep methods, which are
 83 convex combinations of formal forward Euler steps. Thus we only need to discuss the
 84 bound-preserving for one forward Euler step since convex combination can preserve
 85 the bounds.

86 For the numerical tests in this paper, we use a third order explicit SSP Runge-Kutta
 87 method SSPRK(3,3), see [3], which is widely known as the Shu-Osher method, with
 88 SSP coefficient $C = 1$ and effective SSP coefficient $C_{eff} = \frac{1}{3}$. For solving $u_t = F(u)$,
 89 it is given by

$$\begin{aligned}
 & u^{(1)} = u^n, \\
 & u^{(2)} = u^{(1)} + dtF(u^{(1)}), \\
 90 \quad & u^{(3)} = \frac{3}{4}u^{(1)} + \frac{1}{4}(u^{(2)} + F(u^{(2)})), \\
 & u^{n+1} = \frac{1}{3}u^{(1)} + \frac{2}{3}(u^{(3)} + F(u^{(3)})).
 \end{aligned}$$

91 **2.3. A three-point stencil bound-preserving limiter.** In this subsection,
 92 we review the three-point stencil bound-preserving limiter in [5]. Given a sequence of
 93 periodic point values u_i ($i = 1, \dots, N$), $u_0 := u_N$, $u_{N+1} := u_1$ and constant $a \geq 2$,
 94 assume all local weighted averages are in the range $[m, M]$:

$$95 \quad m \leq \frac{1}{a+2}(u_{i-1} + au_i + u_{i+1}) \leq M, \quad i = 1, \dots, N, \quad a \geq 2.$$

96 We separate the point values $\{u_i, i = 1, \dots, N\}$ into two classes of subsets
 97 consisting of consecutive point values. In the following discussion, a *set* refers to
 98 a set of consecutive point values $u_l, u_{l+1}, u_{l+2}, \dots, u_{m-1}, u_m$. For any set $S =$
 99 $\{u_l, u_{l+1}, \dots, u_{m-1}, u_m\}$, we call the first point value u_l and the last point value
 100 u_m as *boundary points*, and call the other point values u_{l+1}, \dots, u_{m-1} as *interior*
 101 *points*. A set of class I is defined as a set satisfying the following:

- 102 1. It contains at least four point values.
 103 2. Both *boundary points* are in $[m, M]$ and all *interior points* are out of range.
 104 3. It contains both undershoot and overshoot points.

105 Notice that in a set of class I, at least one undershoot point is next to an over-
 106 shoot point. For given point values $u_i, i = 1, \dots, N$, suppose all the sets of class I
 107 are $S_1 = \{u_{m_1}, u_{m_1+1}, \dots, u_{n_1}\}$, $S_2 = \{u_{m_2}, \dots, u_{n_2}\}$, \dots , $S_K = \{u_{m_K}, \dots, u_{n_K}\}$,
 108 where $m_1 < m_2 < \dots < m_K$.

109 A set of class II consists of point values between S_i and S_{i+1} and two boundary
 110 points u_{n_i} and $u_{m_{i+1}}$. Namely they are $T_0 = \{u_1, u_2, \dots, u_{m_1}\}$, $T_1 = \{u_{n_1}, \dots, u_{m_2}\}$,
 111 $T_2 = \{u_{n_2}, \dots, u_{m_3}\}$, \dots , $T_K = \{u_{n_K}, \dots, u_N\}$. For periodic data u_i , we can combine
 112 T_K and T_0 to define $T_K = \{u_{n_K}, \dots, u_N, u_1, \dots, u_{m_1}\}$.

113 In the sets of class I, the undershoot and the overshoot are neighbors. In the
 114 sets of class II, the undershoot and the overshoot are separated, i.e., an overshoot is
 115 not next to any undershoot. As a matter of fact, in the numerical tests, the sets of
 116 class I are hardly encountered. Here we include them in the discussion for the sake of
 117 completeness. When there are no sets of class I, all point values form a single set of
 118 class II.

Algorithm 2.1 A bound-preserving limiter for periodic data u_i satisfying $\bar{u}_i \in [m, M]$

Require: the input u_i satisfies $\bar{u}_i = \frac{1}{a+2}(u_{i-1} + au_i + u_{i+1}) \in [m, M]$, $a \geq 2$. Let u_0, u_{N+1} denote u_N, u_1 respectively.

Ensure: the output satisfies $v_i \in [m, M]$, $i = 1, \dots, N$ and $\sum_{i=1}^N v_i = \sum_{i=1}^N u_i$.

1: **Step 0:** First set $v_i = u_i$, $i = 1, \dots, N$. Let v_0, v_{N+1} denote v_N, v_1 respectively.

2: **Step I:** Find all the sets of class I S_1, \dots, S_K (all local saw-tooth profiles) and all the sets of class II T_1, \dots, T_K .

3: **Step II:** For each T_j ($j = 1, \dots, K$),

4: **for** all index i in T_j **do**

5: **if** $u_i < m$ **then**

6: $v_{i-1} \leftarrow v_{i-1} - \frac{(u_{i-1}-m)_+}{(u_{i-1}-m)_+ + (u_{i+1}-m)_+} (m - u_i)_+$

7: $v_{i+1} \leftarrow v_{i+1} - \frac{(u_{i+1}-m)_+}{(u_{i-1}-m)_+ + (u_{i+1}-m)_+} (m - u_i)_+$

8: $v_i \leftarrow m$

9: **end if**

10: **if** $u_i > M$ **then**

11: $v_{i-1} \leftarrow v_{i-1} + \frac{(M-u_{i-1})_+}{(M-u_{i-1})_+ + (M-u_{i+1})_+} (u_i - M)_+$

12: $v_{i+1} \leftarrow v_{i+1} + \frac{(M-u_{i+1})_+}{(M-u_{i-1})_+ + (M-u_{i+1})_+} (u_i - M)_+$

13: $v_i \leftarrow M$

14: **end if**

15: **end for**

16: **Step III:** for each saw-tooth profile $S_j = \{u_{m_j}, \dots, u_{n_j}\}$ ($j = 1, \dots, K$), let N_0 and N_1 be the numbers of undershoot and overshoot points in S_j respectively.

17: Set $U_j = \sum_{i=m_j}^{n_j} v_i$.

18: **for** $i = m_j + 1, \dots, n_j - 1$ **do**

19: **if** $u_i > M$ **then**

20: $v_i \leftarrow M$.

21: **end if**

22: **if** $u_i < m$ **then**

23: $v_i \leftarrow m$.

24: **end if**

25: **end for**

26: Set $V_j = N_1 M + N_0 m + v_{m_j} + v_{n_j}$.

27: Set $A_j = v_{m_j} + v_{n_j} + N_1 M - (N_1 + 2)m$, $B_j = (N_0 + 2)M - v_{m_j} - v_{n_j} - N_0 m$.

28: **if** $V_j - U_j > 0$ **then**

29: **for** $i = m_j, \dots, n_j$ **do**

30: $v_i \leftarrow v_i - \frac{v_i - m}{A_j} (V_j - U_j)$

31: **end for**

32: **else**

33: **for** $i = m_j, \dots, n_j$ **do**

34: $v_i \leftarrow v_i + \frac{M - v_i}{B_j} (U_j - V_j)$

35: **end for**

36: **end if**

119 The algorithm 2.1 can enforce $\bar{u}_i \in [m, M]$ without losing conservation [5]:

120 THEOREM 1. Assume periodic data u_i ($i = 1, \dots, N$) satisfies $\bar{u}_i = \frac{1}{a+2}(u_{i-1} +$
 121 $au_i + u_{i+1}) \in [m, M]$ for some fixed $a \geq 2$ and all $i = 1, \dots, N$ with $u_0 := u_N$ and

122 $u_{N+1} := u_1$, then the output of Algorithm 2.1 satisfies $\sum_{i=1}^N v_i = \sum_{i=1}^N u_i$ and $v_i \in [m, M]$,
 123 $\forall i$.

124 For the two-dimensional case, the same limiter can be used in a dimension by
 125 dimension fashion to enforce $u_{ij} \in [m, M]$.

126 **3. A bound-preserving scheme for the two-dimensional incompressible**
 127 **flow.** In this section we first show the fourth-order compact finite difference with
 128 forward Euler time discretization satisfies the weak monotonicity [5], thus it is bound-
 129 preserving with a naturally constructed discrete divergence-free velocity field.

130 For simplicity, we only consider a periodic boundary condition on a square $[0, 1] \times$
 131 $[0, 1]$. Let $(x_i, y_j) = (\frac{i}{N_x}, \frac{j}{N_y})$ ($i = 1, \dots, N_x, j = 1, \dots, N_y$) be the uniform grid
 132 points on the domain $[0, 1] \times [0, 1]$. All notation in this paper is consistent with those
 133 in [5].

134 **3.1. Weak monotonicity and bound-preserving.** Let $\lambda_1 = \frac{\Delta t}{\Delta x}$ and $\lambda_2 =$
 135 $\frac{\Delta t}{\Delta y}$, the fourth-order compact finite difference scheme with the forward Euler method
 136 for (1.1a) can be given as

$$137 \quad (3.1) \quad \omega_{ij}^{n+1} = \omega_{ij}^n - \lambda_1 [W_{1x}^{-1} D_x(\mathbf{u}^n \circ \omega^n)]_{ij} - \lambda_2 [W_{1y}^{-1} D_y(\mathbf{v}^n \circ \omega^n)]_{ij}.$$

138 With the same notation as in [5], the weighted average in two dimensions can be
 139 denoted as

$$140 \quad (3.2) \quad \bar{\omega} = W_{1x} W_{1y} \omega.$$

141 Then the scheme (3.1) is equivalent to

$$142 \quad \bar{\omega}_{ij}^{n+1} = \bar{\omega}_{ij}^n - \lambda_1 [W_{1y} D_x(\mathbf{u}^n \circ \omega^n)]_{ij} - \lambda_2 [W_{1x} D_y(\mathbf{v}^n \circ \omega^n)]_{ij}$$

$$143 \quad (3.3) \quad = \frac{1}{36} \begin{pmatrix} 1 & 4 & 1 \\ 4 & 16 & 4 \\ 1 & 4 & 1 \end{pmatrix} : \Omega^n - \frac{\lambda_1}{12} \begin{pmatrix} -1 & 0 & 1 \\ -4 & 0 & 4 \\ -1 & 0 & 1 \end{pmatrix} : (U^n \circ \Omega^n) - \frac{\lambda_2}{12} \begin{pmatrix} 1 & 4 & 1 \\ 0 & 0 & 0 \\ -1 & -4 & -1 \end{pmatrix} : (V^n \circ \Omega^n),$$

145 where \circ denotes the matrix Hadamard product, and

$$146 \quad U = \begin{pmatrix} u_{i-1,j+1} & u_{i,j+1} & u_{i+1,j+1} \\ u_{i-1,j} & u_{i,j} & u_{i+1,j} \\ u_{i-1,j-1} & u_{i,j-1} & u_{i+1,j-1} \end{pmatrix}, V = \begin{pmatrix} v_{i-1,j+1} & v_{i,j+1} & v_{i+1,j+1} \\ v_{i-1,j} & v_{i,j} & v_{i+1,j} \\ v_{i-1,j-1} & v_{i,j-1} & v_{i+1,j-1} \end{pmatrix},$$

$$147 \quad \Omega = \begin{pmatrix} \omega_{i-1,j+1} & \omega_{i,j+1} & \omega_{i+1,j+1} \\ \omega_{i-1,j} & \omega_{i,j} & \omega_{i+1,j} \\ \omega_{i-1,j-1} & \omega_{i,j-1} & \omega_{i+1,j-1} \end{pmatrix}.$$

149 It is straightforward to verify the *weak monotonicity*, i.e., $\bar{\omega}_{ij}^{n+1}$ is a monotonically
 150 increasing function with respect to all point values ω_{ij}^n involved in (3.3) under the
 151 CFL condition

$$152 \quad \frac{\Delta t}{\Delta x} \max_{ij} |u_{ij}^n| + \frac{\Delta t}{\Delta y} \max_{ij} |v_{ij}^n| \leq \frac{1}{3}.$$

153 However, the monotonicity is sufficient for bound-preserving $\bar{\omega}_{ij}^{n+1} \in [m, M]$, only if
 154 the following consistency condition holds:

$$155 \quad (3.4) \quad \omega_{ij}^n \equiv m \Rightarrow \bar{\omega}_{ij}^{n+1} = m, \quad \omega_{ij}^n \equiv M \Rightarrow \bar{\omega}_{ij}^{n+1} = M.$$

156 Plugging $\omega_{ij}^n \equiv m$ in (3.3), we get

$$157 \quad \bar{\omega}_{ij}^{n+1} = m \left(1 - \lambda_1 (W_{1y} D_x \mathbf{u}^n)_{ij} - \lambda_2 (W_{1x} D_y \mathbf{v}^n)_{ij} \right).$$

158 Thus the consistency (3.4) holds only if the velocity $\langle \mathbf{u}^n, \mathbf{v}^n \rangle$ satisfies:

$$159 \quad (3.5) \quad \frac{1}{\Delta x} D_x W_{1y} \mathbf{u}^n + \frac{1}{\Delta x} D_y W_{1x} \mathbf{v}^n = 0.$$

160 Therefore we have the following bound-preserving result:

161 **THEOREM 2.** *If the velocity $\langle \mathbf{u}^n, \mathbf{v}^n \rangle$ satisfies the discrete divergence free con-*
 162 *straint (3.5) and $\omega_{ij}^n \in [m, M]$, then under the CFL constraint*

$$163 \quad \frac{\Delta t}{\Delta x} \max_{ij} |u_{ij}^n| + \frac{\Delta t}{\Delta y} \max_{ij} |v_{ij}^n| \leq \frac{1}{3},$$

164 *the scheme (3.3) satisfies $\bar{\omega}_{ij}^{n+1} \in [m, M]$.*

165 **3.2. A discrete divergence free velocity field.** In the following discussion,
 166 we may discard the superscript n for convenience assuming everything discussed is at
 167 time step n .

168 Note that (3.5) is a discrete divergence free constraint and we can construct a
 169 fourth-order accurate velocity field satisfying (3.5). Given ω_{ij} , we first compute ψ_{ij}
 170 by a fourth-order compact finite difference scheme for the Poisson equation (1.1b).
 171 The detail of the Poisson solvers including the fast Poisson solver is given in the
 172 appendices.

173 With the fourth-order compact finite difference we have

$$174 \quad (3.6) \quad -\frac{1}{\Delta y} D_y \Psi = W_{1y} \mathbf{u}, \quad \frac{1}{\Delta x} D_x \Psi = W_{1x} \mathbf{v},$$

where

$$\Psi = \begin{pmatrix} \psi_{11} & \psi_{12} & \cdots & \psi_{1,N_y} \\ \psi_{21} & \psi_{22} & \cdots & \psi_{2,N_y} \\ \vdots & \vdots & \ddots & \vdots \\ \psi_{N_x-1,1} & \psi_{N_x-1,2} & \cdots & \psi_{N_x-1,N_y} \\ \psi_{N_x,1} & \psi_{N_x,2} & \cdots & \psi_{N_x,N_y} \end{pmatrix}_{N_x \times N_y}.$$

175 Since the two finite difference operators D_x and D_y commute, it is straightforward to
 176 verify that the velocity field computed by (3.6) satisfies (3.5).

177 **3.3. A fourth-order accurate bound-preserving scheme.** For the Euler
 178 equations (1.1), the following implementation of the fourth-order compact finite dif-
 179 ference with forward Euler time discretization scheme can preserve the bounds:

- 180 1. Given $\omega_{ij}^n \in [m, M]$, solve the Poisson equation (1.1b) by the fourth-order
 181 accurate compact finite difference scheme to obtain point values of the stream
 182 function ψ_{ij} .
- 183 2. Construct \mathbf{u} and \mathbf{v} by (3.6).
- 184 3. Obtain $\bar{\omega}_{ij}^{n+1} \in [m, M]$ by scheme (3.3).
- 185 4. Apply the limiting procedure in Section 2.3 to obtain $\omega_{ij}^{n+1} \in [m, M]$.

186 For high order SSP time discretizations, we should use the same implementation above
187 for each time stage or time step.

188 For the Navier-Stokes equations (1.2), with $\mu_1 = \frac{\Delta t}{\Delta x^2}$ and $\mu_2 = \frac{\Delta t}{\Delta y^2}$, the scheme
189 can be written as

$$190 \quad (3.7) \quad \begin{aligned} \omega_{ij}^{n+1} = & \omega_{ij}^n - \lambda_1 [W_{1x}^{-1} D_x(\mathbf{u}^n \circ \boldsymbol{\omega}^n)]_{ij} - \lambda_2 [W_{1y}^{-1} D_y(\mathbf{v}^n \circ \boldsymbol{\omega}^n)]_{ij} \\ & + \frac{\mu_1}{Re} W_{2x}^{-1} D_{xx} \omega_{ij}^n + \frac{\mu_2}{Re} W_{2y}^{-1} D_{yy} \omega_{ij}^n, \end{aligned}$$

191 In a manner similar to (3.2), we define

$$192 \quad (3.8) \quad \tilde{\omega} := W_{2x} W_{2y} \omega,$$

with $W_1 := W_{1x} W_{1y}$ and $W_2 := W_{2x} W_{2y}$. Due to definition (3.2) and the fact
operators W_1 and W_2 commute, i.e. $W_1 W_2 = W_2 W_1$, we have

$$\tilde{\tilde{\omega}} = W_2 W_1 \omega = W_1 W_2 \omega = \tilde{\omega}.$$

193 Then scheme (3.7) is equivalent to

$$194 \quad (3.9) \quad \begin{aligned} \tilde{\tilde{\omega}}_{ij}^{n+1} = & \tilde{\tilde{\omega}}_{ij}^n - \frac{\lambda_1}{12} [W_2 W_{1y} D_x(\mathbf{u}^n \circ \boldsymbol{\omega}^n)]_{ij} - \frac{\lambda_2}{12} [W_2 W_{1x} D_y(\mathbf{v}^n \circ \boldsymbol{\omega}^n)]_{ij} \\ & + \frac{\mu_1}{Re} W_1 W_{2y} D_{xx} \omega_{ij}^n + \frac{\mu_2}{Re} W_1 W_{2x} D_{yy} \omega_{ij}^n. \end{aligned}$$

195 Following the discussion in Section 3.1 and the discussion for the two-dimensional
196 convection-diffusion in [5], we have the following result:

THEOREM 3. *If the velocity $\langle \mathbf{u}^n, \mathbf{v}^n \rangle$ satisfies the constraint (3.5) and $\omega_{ij}^n \in [m, M]$, then under the CFL constraint*

$$\frac{\Delta t}{\Delta x} \max_{ij} |u_{ij}^n| + \frac{\Delta t}{\Delta y} \max_{ij} |v_{ij}^n| \leq \frac{1}{6}, \quad \frac{\Delta t}{Re \Delta x^2} + \frac{\Delta t}{Re \Delta y^2} \leq \frac{5}{24},$$

197 *the scheme (3.9) satisfies $\tilde{\tilde{\omega}}_{ij}^{n+1} \in [m, M]$.*

198 Given $\tilde{\tilde{\omega}}_{ij}$, we can recover point values ω_{ij} by obtaining first $\tilde{\omega}_{ij} = W_1^{-1} \tilde{\tilde{\omega}}_{ij}$ then
199 $\omega_{ij} = W_2^{-1} \tilde{\omega}_{ij}$. Given point values ω_{ij} satisfying $\tilde{\tilde{\omega}}_{ij} \in [m, M]$ for any i and j , we can
200 use the limiter in Algorithm 2.1 in a dimension by dimension fashion several times to
201 enforce $\omega_{ij} \in [m, M]$:

- 202 1. Given $\tilde{\tilde{\omega}}_{ij} \in [m, M]$, compute $\tilde{\omega}_{ij} = W_1^{-1} \tilde{\tilde{\omega}}_{ij}$ and apply the limiting Algorithm
203 2.1 with $a = 4$ in both x -direction and y -direction to ensure $\tilde{\omega}_{ij} \in [m, M]$.
- 204 2. Given $\tilde{\omega}_{ij} \in [m, M]$, compute $\omega_{ij} = W_2^{-1} \tilde{\omega}_{ij}$ and apply the limiting algorithm
205 Algorithm 2.1 with $a = 10$ in both x -direction and y -direction to ensure
206 $\omega_{ij} \in [m, M]$.

207 **4. A TVB limiter for the two-dimensional incompressible flow.** To have
208 nonlinear stability and eliminate oscillations for shocks, a TVBM (total variation
209 bounded in the means) limiter was introduced for the compact finite difference scheme
210 solving scalar convection equations in [2]. In this section, we will modify this limiter
211 for the incompressible flow so that it does not affect the bound-preserving property.
212 Thus we can use both the TVB limiter and the bound-preserving limiter in Algorithm
213 2.1 to preserve bounds while reducing oscillations. For simplicity, we only consider
214 the numerical scheme for the incompressible Euler equations (1.1). In this section, we
215 may discard the superscript n if a variable is defined at time step n .

216 **4.1. The TVB limiter.** The scheme (3.3) can be written in a conservative form:

$$217 \quad (4.1) \quad \bar{\omega}_{ij}^{n+1} = \bar{\omega}_{ij}^n - \lambda_1[(\hat{u}\omega)_{i+\frac{1}{2},j}^n - (\hat{u}\omega)_{i-\frac{1}{2},j}^n] - \lambda_2[(\hat{v}\omega)_{i,j+\frac{1}{2}}^n - (\hat{v}\omega)_{i,j-\frac{1}{2}}^n],$$

218 involving a numerical flux $(\hat{u}\omega)_{i+\frac{1}{2},j}^n$ and $(\hat{v}\omega)_{i,j+\frac{1}{2}}^n$ as local functions of u_{kl}^n , v_{kl}^n and
219 ω_{kl}^n . The numerical flux is defined as

$$220 \quad (4.2) \quad \begin{aligned} (\hat{u}\omega)_{i+\frac{1}{2},j} &= \frac{1}{2} ([W_{1y}(\mathbf{u} \circ \omega)]_{ij} + [W_{1y}(\mathbf{u} \circ \omega)]_{i+1,j}), \\ (\hat{v}\omega)_{i,j+\frac{1}{2}} &= \frac{1}{2} ([W_{1x}(\mathbf{v} \circ \omega)]_{ij} + [W_{1x}(\mathbf{v} \circ \omega)]_{i,j+1}). \end{aligned}$$

221 Similarly we denote

$$222 \quad (4.3) \quad \begin{aligned} \hat{u}_{i+\frac{1}{2},j} &= \frac{1}{2} \left((W_{1y}\mathbf{u})_{ij} + (W_{1y}\mathbf{u})_{i+1,j} \right), \\ \hat{v}_{i,j+\frac{1}{2}} &= \frac{1}{2} \left((W_{1x}\mathbf{v})_{ij} + (W_{1x}\mathbf{v})_{i,j+1} \right). \end{aligned}$$

223 The limiting is defined in a dimension by dimension manner. For the flux splitting,
224 it is done as in one-dimension. Consider a splitting of u satisfying

$$225 \quad (4.4) \quad u^+ \geq 0, \quad u^- \leq 0.$$

The simplest such splitting is the Lax-Friedrichs splitting

$$u^\pm = \frac{1}{2}(u \pm \alpha), \quad \alpha = \max_{(x,y) \in \Omega} |u(x,y)|.$$

226 Then we have

$$227 \quad u = u^+ + u^-, \quad u\omega = u^+\omega + u^-\omega,$$

228 and we write the flux $(\hat{u}\omega)_{i+\frac{1}{2},j}$ and $\hat{u}_{i+\frac{1}{2},j}$ as

$$229 \quad (\hat{u}\omega)_{i+\frac{1}{2},j} = (\hat{u}\omega)_{i+\frac{1}{2},j}^+ + (\hat{u}\omega)_{i+\frac{1}{2},j}^-, \quad \hat{u}_{i+\frac{1}{2},j} = \hat{u}_{i+\frac{1}{2},j}^+ + \hat{u}_{i+\frac{1}{2},j}^-$$

230 where $(\hat{u}\omega)_{i+\frac{1}{2},j}^\pm$ and $\hat{u}_{i+\frac{1}{2},j}^\pm$ are obtained by adding superscripts \pm to u_{ij} in (4.2) and
231 (4.3) respectively, i.e.

$$232 \quad \begin{aligned} (\hat{u}\omega)_{i+\frac{1}{2},j}^\pm &= \frac{1}{2} ([W_{1y}(\mathbf{u}^\pm \circ \omega)]_{ij} + [W_{1y}(\mathbf{u}^\pm \circ \omega)]_{i+1,j}), \\ \hat{u}_{i+\frac{1}{2},j}^\pm &= \frac{1}{2} \left((W_{1y}\mathbf{u}^\pm)_{ij} + (W_{1y}\mathbf{u}^\pm)_{i+1,j} \right), \end{aligned}$$

233 where $\mathbf{u}^\pm = (u_{ij}^\pm)$. With a dummy index j referring y value, we first take the differ-
234 ences between the high-order numerical flux and the first-order upwind flux

$$237 \quad (4.5) \quad d(\hat{u}\omega)_{i+\frac{1}{2},j}^+ = (\hat{u}\omega)_{i+\frac{1}{2},j}^+ - u_{i+\frac{1}{2},j}^+ \bar{\omega}_{ij}, \quad d(\hat{u}\omega)_{i+\frac{1}{2},j}^- = u_{i+\frac{1}{2},j}^- \bar{\omega}_{i+1,j} - (\hat{u}\omega)_{i+\frac{1}{2},j}^-.$$

238 Limit them by

$$239 \quad (4.6) \quad \begin{aligned} d(\hat{u}\omega)_{i+\frac{1}{2},j}^{+(m)} &= m \left(d(\hat{u}\omega)_{i+\frac{1}{2},j}^+, u_{i+\frac{1}{2},j}^+ \Delta_+^x \bar{\omega}_{ij}, u_{i-\frac{1}{2},j}^+ \Delta_+^x \bar{\omega}_{i-1,j} \right), \\ d(\hat{u}\omega)_{i+\frac{1}{2},j}^{-(m)} &= m \left(d(\hat{u}\omega)_{i+\frac{1}{2},j}^-, u_{i+\frac{1}{2},j}^- \Delta_+^x \bar{\omega}_{ij}, u_{i+\frac{3}{2},j}^- \Delta_+^x \bar{\omega}_{i+1,j} \right), \end{aligned}$$

240 where $\Delta_+^x v_{ij} \equiv v_{i+1,j} - v_{ij}$ is the forward difference operator in the x direction, and
 241 m is the standard *minmod* function

$$242 \quad (4.7) \quad m(a_1, \dots, a_k) = \begin{cases} s \min_{1 \leq i \leq k} |a_i|, & \text{if } \text{sign}(a_1) = \dots = \text{sign}(a_k) = s, \\ 0, & \text{otherwise.} \end{cases}$$

243 As mentioned in [2], the limiting defined in (4.6) maintains the formal accuracy
 244 of the compact schemes in smooth regions of the solution with the assumption

$$245 \quad (4.8) \quad \bar{\omega}_{ij} = (W_{1x} W_{1y} \omega)_{ij} = \omega_{ij} + \mathcal{O}(\Delta x^2) \text{ for } \omega \in C^2.$$

246 Under the assumption (4.8), by simple Taylor expansion,

$$247 \quad (4.9) \quad \begin{aligned} d(\hat{u}\omega)_{i+\frac{1}{2},j}^\pm &= \frac{1}{2} u_{i+\frac{1}{2},j}^\pm \omega_{x,ij} \Delta x + \mathcal{O}(\Delta x^2), \\ u_{k+\frac{1}{2},j}^\pm \Delta_+^x \bar{\omega}_{kj} &= u_{i+\frac{1}{2},j}^\pm \omega_{x,ij} \Delta x + \mathcal{O}(\Delta x^2), \quad k = i-1, i, i+1. \end{aligned}$$

Hence in smooth regions away from critical points of ω , for sufficiently small Δx , the minmod function (4.7) will pick the first argument, yielding

$$d(\hat{u}\omega)_{i+\frac{1}{2},j}^{\pm(m)} = d(\hat{u}\omega)_{i+\frac{1}{2},j}^\pm.$$

248 Since the accuracy may degenerate to first-order at critical points, as a remedy, the
 249 modified *minmod* function [7, 1] is introduced

$$250 \quad (4.10) \quad \tilde{m}(a_1, \dots, a_k) = \begin{cases} a_1, & \text{if } |a_1| \leq P\Delta x^2, \\ m(a_1, \dots, a_k), & \text{otherwise,} \end{cases}$$

251 where P is a positive constant independent of Δx and m is the standard *minmod*
 252 function (4.7). See more detailed discussion in [2].

253 Then we obtain the limited numerical fluxes as

$$254 \quad (4.11) \quad (\hat{u}\omega)_{i+\frac{1}{2},j}^{+(m)} = u_{i+\frac{1}{2},j}^+ \bar{\omega}_{ij} + d(\hat{u}\omega)_{i+\frac{1}{2},j}^{+(m)}, \quad (\hat{u}\omega)_{i+\frac{1}{2},j}^{-(m)} = u_{i+\frac{1}{2},j}^- \bar{\omega}_{i+1,j} - d(\hat{u}\omega)_{i+\frac{1}{2},j}^{-(m)}.$$

255 and

$$256 \quad (4.12) \quad (\hat{u}\omega)_{i+\frac{1}{2},j}^{(m)} = (\hat{u}\omega)_{i+\frac{1}{2},j}^{+(m)} + (\hat{u}\omega)_{i+\frac{1}{2},j}^{-(m)}$$

257 The flux in the y -direction can be defined analogously.

258 The following result was proven in [2]:

LEMMA 4.1. *For any n and Δt such that $0 \leq n\Delta t \leq T$, scheme (4.1) with flux (4.12) satisfies a maximum principle in the means:*

$$\max_{i,j} |\bar{\omega}_{ij}^{n+1}| \leq \max_{i,j} |\bar{\omega}_{ij}^n|$$

under the CFL condition

$$\left[\max(u^+) + \max(-u^-) \right] \frac{\Delta t}{\Delta x} + \left[\max(v^+) + \max(-v^-) \right] \frac{\Delta t}{\Delta y} \leq \frac{1}{2}$$

259 where the maximum is taken in $\min_{i,j} u_{ij}^n \leq u \leq \max_{i,j} u_{ij}^n$, $\min_{i,j} v_{ij}^n \leq v \leq \max_{i,j} v_{ij}^n$. ■

260 **4.2. The bound-preserving property of the nonlinear scheme with mod-**
 261 **ified flux.** The compact finite difference scheme with the TVB limiter in the last
 262 section is

$$263 \quad (4.13) \quad \bar{\omega}_{ij}^{n+1} = \bar{\omega}_{ij}^n - \lambda_1 \left((\hat{u}\omega)_{i+\frac{1}{2},j}^{(m)} - (\hat{u}\omega)_{i-\frac{1}{2},j}^{(m)} \right) - \lambda_2 \left((\hat{v}\omega)_{i,j+\frac{1}{2}}^{(m)} - (\hat{v}\omega)_{i,j-\frac{1}{2}}^{(m)} \right),$$

264 where the numerical flux $(\hat{u}\omega)_{i+\frac{1}{2},j}^{(m)}$, $(\hat{u}\omega)_{i,j+\frac{1}{2}}^{(m)}$ is the modified flux approximating
 265 (4.2).

266 **THEOREM 4.** *If $\omega_{ij}^n \in [m, M]$, under the CFL condition*

$$267 \quad (4.14) \quad \lambda_1 \max_{i,j} |u_{ij}^{(\pm)}| \leq \frac{1}{24}, \quad \lambda_2 \max_{i,j} |v_{ij}^{(\pm)}| \leq \frac{1}{24},$$

268 *the nonlinear scheme (4.13) satisfies*

$$269 \quad \bar{\omega}_{ij}^{n+1} \in [m, M].$$

270 *Proof.* We have

$$\begin{aligned} & (4.15) \quad \bar{\omega}_{ij}^{n+1} = \bar{\omega}_{ij}^n - \lambda_1 \left((\hat{u}\omega)_{i+\frac{1}{2},j}^{(m)} - (\hat{u}\omega)_{i-\frac{1}{2},j}^{(m)} \right) - \lambda_2 \left((\hat{v}\omega)_{i,j+\frac{1}{2}}^{(m)} - (\hat{v}\omega)_{i,j-\frac{1}{2}}^{(m)} \right) \\ & = \frac{1}{8} \left((\bar{\omega}_{ij}^n - 8\lambda_1(\hat{u}\omega)_{i+\frac{1}{2},j}^{+(m)}) + (\bar{\omega}_{ij}^n - 8\lambda_1(\hat{u}\omega)_{i+\frac{1}{2},j}^{- (m)}) + (\bar{\omega}_{ij}^n + 8\lambda_1(\hat{u}\omega)_{i-\frac{1}{2},j}^{+(m)}) + (\bar{\omega}_{ij}^n + 8\lambda_1(\hat{u}\omega)_{i-\frac{1}{2},j}^{- (m)}) \right. \\ & \quad \left. + (\bar{\omega}_{ij}^n - 8\lambda_2(\hat{v}\omega)_{i,j+\frac{1}{2}}^{+(m)}) + (\bar{\omega}_{ij}^n - 8\lambda_2(\hat{v}\omega)_{i,j+\frac{1}{2}}^{- (m)}) + (\bar{\omega}_{ij}^n + 8\lambda_2(\hat{v}\omega)_{i,j-\frac{1}{2}}^{+(m)}) + (\bar{\omega}_{ij}^n + 8\lambda_2(\hat{v}\omega)_{i,j-\frac{1}{2}}^{- (m)}) \right). \end{aligned}$$

272 Under the CFL condition (4.14), we will prove that the eight terms satisfy the
 273 following bounds

$$\begin{aligned} & \bar{\omega}_{ij}^n - 8\lambda_1(\hat{u}\omega)_{i+\frac{1}{2},j}^{+(m)} \in \left[m - 8\lambda_1\hat{u}_{i+\frac{1}{2},j}^+ m, M - 8\lambda_1\hat{u}_{i+\frac{1}{2},j}^+ M \right], \\ & \bar{\omega}_{ij}^n - 8\lambda_1(\hat{u}\omega)_{i+\frac{1}{2},j}^{- (m)} \in \left[m - 8\lambda_1\hat{u}_{i+\frac{1}{2},j}^- m, M - 8\lambda_1\hat{u}_{i+\frac{1}{2},j}^- M \right], \\ & \bar{\omega}_{ij}^n + 8\lambda_1(\hat{u}\omega)_{i-\frac{1}{2},j}^{+(m)} \in \left[m + 8\lambda_1\hat{u}_{i-\frac{1}{2},j}^+ m, M + 8\lambda_1\hat{u}_{i-\frac{1}{2},j}^+ M \right], \\ & \bar{\omega}_{ij}^n + 8\lambda_1(\hat{u}\omega)_{i-\frac{1}{2},j}^{- (m)} \in \left[m + 8\lambda_1\hat{u}_{i-\frac{1}{2},j}^- m, M + 8\lambda_1\hat{u}_{i-\frac{1}{2},j}^- M \right], \\ & \bar{\omega}_{ij}^n - 8\lambda_2(\hat{v}\omega)_{i,j+\frac{1}{2}}^{+(m)} \in \left[m - 8\lambda_2\hat{v}_{i,j+\frac{1}{2}}^+ m, M - 8\lambda_2\hat{v}_{i,j+\frac{1}{2}}^+ M \right], \\ & \bar{\omega}_{ij}^n - 8\lambda_2(\hat{v}\omega)_{i,j+\frac{1}{2}}^{- (m)} \in \left[m - 8\lambda_2\hat{v}_{i,j+\frac{1}{2}}^- m, M - 8\lambda_2\hat{v}_{i,j+\frac{1}{2}}^- M \right], \\ & \bar{\omega}_{ij}^n + 8\lambda_2(\hat{v}\omega)_{i,j-\frac{1}{2}}^{+(m)} \in \left[m + 8\lambda_2\hat{v}_{i,j-\frac{1}{2}}^+ m, M + 8\lambda_2\hat{v}_{i,j-\frac{1}{2}}^+ M \right], \\ & \bar{\omega}_{ij}^n + 8\lambda_2(\hat{v}\omega)_{i,j-\frac{1}{2}}^{- (m)} \in \left[m + 8\lambda_2\hat{v}_{i,j-\frac{1}{2}}^- m, M + 8\lambda_2\hat{v}_{i,j-\frac{1}{2}}^- M \right]. \end{aligned}$$

275 For (4.16), by taking the sum of the lower bounds and upper bounds and multi-
 276 plying them by $\frac{1}{8}$, we obtain

$$277 \quad (4.17) \quad \bar{\omega}_{ij}^{n+1} \in [m - mO_{ij}, M - MO_{ij}],$$

278 with

$$\begin{aligned}
O_{ij} &= \lambda_1(\hat{u}_{i+\frac{1}{2},j} - \hat{u}_{i-\frac{1}{2},j}) - \lambda_2(\hat{u}_{i,j+\frac{1}{2}} - \hat{u}_{i,j-\frac{1}{2}}) \\
(4.18) \quad &= \frac{\lambda_1}{2} ((W_{1y}\mathbf{u})_{i+1,j} - (W_{1y}\mathbf{u})_{i-1,j}) + \frac{\lambda_2}{2} ((W_{1y}\mathbf{v})_{i,j+1} - (W_{1y}\mathbf{v})_{i,j-1}) \\
&= \frac{\Delta t}{2} (D_x W_{1y}\mathbf{u} + D_y W_{1x}\mathbf{v}) = 0.
\end{aligned}$$

280 Therefore, we conclude $\bar{\omega}_{ij}^{n+1} \in [m, M]$.

281 We only discuss the first two term in (4.16) since the proof for the rest is similar.
 282 By the definition of the modified *minmod* function (4.10) and (4.11), we have

$$\begin{aligned}
(4.19) \quad & (\hat{u}\omega)_{i+\frac{1}{2},j}^{+(m)} \in \left[\min\{(\hat{u}\omega)_{i+\frac{1}{2},j}^+, u_{i+\frac{1}{2},j}^+ \bar{\omega}_{ij}\}, \max\{(\hat{u}\omega)_{i+\frac{1}{2},j}^+, u_{i+\frac{1}{2},j}^+ \bar{\omega}_{ij}\} \right], \\
& (\hat{u}\omega)_{i+\frac{1}{2},j}^{-(m)} \in \left[\min\{(\hat{u}\omega)_{i+\frac{1}{2},j}^-, u_{i+\frac{1}{2},j}^- \bar{\omega}_{i+1,j}\}, \max\{(\hat{u}\omega)_{i+\frac{1}{2},j}^-, u_{i+\frac{1}{2},j}^- \bar{\omega}_{i+1,j}\} \right].
\end{aligned}$$

284 We notice that under CFL condition (4.14),

$$(4.20) \quad \bar{\omega}_{ij}^n - 8\lambda_1(\hat{u}\omega)_{i+\frac{1}{2},j}^+, \quad \bar{\omega}_{ij}^n - 8\lambda_1 u_{i+\frac{1}{2},j}^+ \bar{\omega}_{ij}^n, \quad \bar{\omega}_{ij}^n - 8\lambda_1(\hat{u}\omega)_{i+\frac{1}{2},j}^-$$

286 are all monotonically increasing functions with respect to variables ω_{kj}^n , $k = i-1, i, i+1$. Due to the flux splitting (4.4),

$$(4.21) \quad \bar{\omega}_{ij}^n - 8\lambda_1 u_{i+\frac{1}{2},j}^- \bar{\omega}_{i+1,j}^n$$

289 is also a monotonically increasing function with respect to variables ω_{kj}^n , $k = i-1, i, i+1, i+2$. Therefore, with the assumption $\omega_{ij}^n \in [m, M]$, we obtain

$$\begin{aligned}
(4.22) \quad & \bar{\omega}_{ij}^n - 8\lambda_1(\hat{u}\omega)_{i+\frac{1}{2},j}^+, \quad \bar{\omega}_{ij}^n - 8\lambda_1 u_{i+\frac{1}{2},j}^+ \bar{\omega}_{ij}^n \in \left[m - 8\lambda_1 \hat{u}_{i+\frac{1}{2},j}^+, M - 8\lambda_1 \hat{u}_{i+\frac{1}{2},j}^+ M \right], \\
& \bar{\omega}_{ij}^n - 8\lambda_1(\hat{u}\omega)_{i+\frac{1}{2},j}^-, \quad \bar{\omega}_{ij}^n - 8\lambda_1 u_{i+\frac{1}{2},j}^- \bar{\omega}_{i+1,j}^n \in \left[m - 8\lambda_1 \hat{u}_{i+\frac{1}{2},j}^-, M - 8\lambda_1 \hat{u}_{i+\frac{1}{2},j}^- M \right],
\end{aligned}$$

292 with (4.19), which implies the first two terms of (4.16). \square

293 **REMARK 1.** *We remark here the above proof is independent of the second and*
 294 *third arguments of the minmod function (4.10). Therefore, the proof hold for other*
 295 *limiters with different second and third arguments in the same minmod function*
 296 *(4.10).*

297 **REMARK 2.** *The TVB limiter in this paper is designed to modify the convection*
 298 *flux only thus it also applies to the Navier-Stokes equation. Moreover, under suitable*
 299 *CFL condition, the full scheme with TVB limiter can still preserve $\bar{\omega}_{ij}^{n+1} \in [m, M]$*
 300 *with $\omega_{ij}^n \in [m, M]$.*

301 **4.3. An alternative TVB limiter.** Another TVB limiter can be defined by
 302 replacing (4.6) with

$$\begin{aligned}
(4.23) \quad & d(\hat{u}\omega)_{i+\frac{1}{2},j}^{+(m)} = m \left(d(\hat{u}\omega)_{i+\frac{1}{2},j}^+, \Delta_x^+(u_{i+\frac{1}{2},j}^+ \bar{\omega}_{ij}), \Delta_x^+(u_{i-\frac{1}{2},j}^+ \bar{\omega}_{i-1,j}) \right), \\
& d(\hat{u}\omega)_{i+\frac{1}{2},j}^{-(m)} = m \left(d(\hat{u}\omega)_{i+\frac{1}{2},j}^-, \Delta_x^+(u_{i-\frac{1}{2},j}^- \bar{\omega}_{i,j}), \Delta_x^+(u_{i+\frac{1}{2},j}^- \bar{\omega}_{i+1,j}) \right).
\end{aligned}$$

304 All the other procedures in the limiter are exactly the same as in Section 4.1. The
 305 limiter does not affect the bound-preserving property due to the arguments in Remark
 306 1.

307 **5. Numerical Tests.** In this subsection, we test the fourth-order compact finite
 308 difference scheme with both the bound-preserving and the TVB limiter for the two-
 309 dimensional incompressible flow.

310 In the numerical test, we refer to the bound-preserving limiter as BP, the TVB
 311 limiter in Section 4.1 as TVB1, and the TVB limiter in section 4.3 as TVB2. The
 312 parameter in the minmod function used in TVB limiters is denoted as P. In all the
 313 following numerical tests, we use SSPRK(3,3) as mentioned in section 2.2.

314 **5.1. Accuracy Test.** For the Euler Equation (1.1) with periodic boundary con-
 315 dition and initial data $\omega(x, y, 0) = -2 \sin(2x) \sin(y)$ on the domain $[0, 2\pi] \times [0, 2\pi]$, the
 316 exact solution is $\omega(x, y, t) = -2 \sin(2x) \sin(y)$. We test the accuracy of the proposed
 317 scheme on this solution. The errors for $P = 300$ are given in Table 1, and we observe
 the designed order of accuracy for this special steady state solution.

Table 1: Incompressible Euler equations. Fourth-order compact FD for vorticity,
 $t = 0.5$. With BP and TVB1 limiters, $P = 300$.

$N \times N$	L^2 error	order	L^∞ error	order
32×32	3.16E-3	-	1.00E-3	-
64×64	1.86E-4	4.09	5.90E-5	4.09
128×128	1.14E-5	4.02	3.63E-6	4.02
256×256	7.13E-7	4.01	2.67E-7	4.00

318

5.2. Double Shear Layer Problem. We test the scheme for the double shear
 layer problem on the domain $[0, 2\pi] \times [0, 2\pi]$ with a periodic boundary condition. The
 initial condition is

$$\omega(x, y, 0) = \begin{cases} \delta \cos(x) - \frac{1}{\rho} \operatorname{sech}^2((y - \frac{\pi}{2})/\rho), & y \leq \pi \\ \delta \cos(x) + \frac{1}{\rho} \operatorname{sech}^2((\frac{3\pi}{2} - y)/\rho), & y > \pi \end{cases}$$

319 with $\delta = 0.05$ and $\rho = \pi/15$. The vorticity ω at time $T = 6$ and $T = 8$ are shown in
 320 Figure 1, Figure 2 and Figure 3. With both the bound-preserving limiter and TVB
 321 limiter, the numerical solutions are ensured to be in the range $[-\delta - \frac{1}{\rho}, \delta + \frac{1}{\rho}]$. The
 322 TVB limiter can also reduce oscillations.

5.3. Vortex Patch Problem. We test the limiters for the vortex patch prob-
 lem in the domain $[0, 2\pi] \times [0, 2\pi]$ with a periodic boundary condition. The initial
 condition is

$$\omega(x, y, 0) = \begin{cases} -1, & (x, y) \in [\frac{\pi}{2}, \frac{3\pi}{2}] \times [\frac{\pi}{4}, \frac{3\pi}{4}]; \\ 1, & (x, y) \in [\frac{\pi}{2}, \frac{3\pi}{2}] \times [\frac{5\pi}{4}, \frac{7\pi}{4}]; \\ 0, & \text{otherwise.} \end{cases}$$

323 Numerical solutions for incompressible Euler are shown in Figure 4, Figure 5, Figure
 324 6 and Figure 7. We can observe that the solutions generated by the compact finite
 325 difference scheme with only the bound-preserving limiter are still highly oscillatory
 326 for the Euler equation without the TVB limiter.

327 Notice that the oscillations in Figure 4 suggest that the artificial viscosity induced
 328 by the bound-preserving limiter is quite low.

329 **6. Concluding Remarks.** We have proven that a simple limiter can preserve
 330 bounds for the fourth-order compact finite difference method solving the two dimen-
 331 sional incompressible Euler equation, with a discrete divergence-free velocity field.

332 We also prove that the TVB limiter modified from [2] does not affect the bound-
333 preserving property of $\bar{\omega}$. With both the TVB limiter and the bound-preserving
334 limiter, the numerical solutions of high order compact finite difference scheme can be
335 rendered non-oscillatory and strictly bound-preserving.

336 For the sixth-order and eighth-order compact finite difference method for con-
337 vection problem with weak monotonicity in [5], the divergence-free velocity can be
338 constructed accordingly, which gives a higher order bound-preserving scheme for the
339 incompressible flow by applying Algorithm 2.1 for several times. The TVB limiting
340 procedure in Section 4.1 can also be defined with a similar result as Theorem 4.

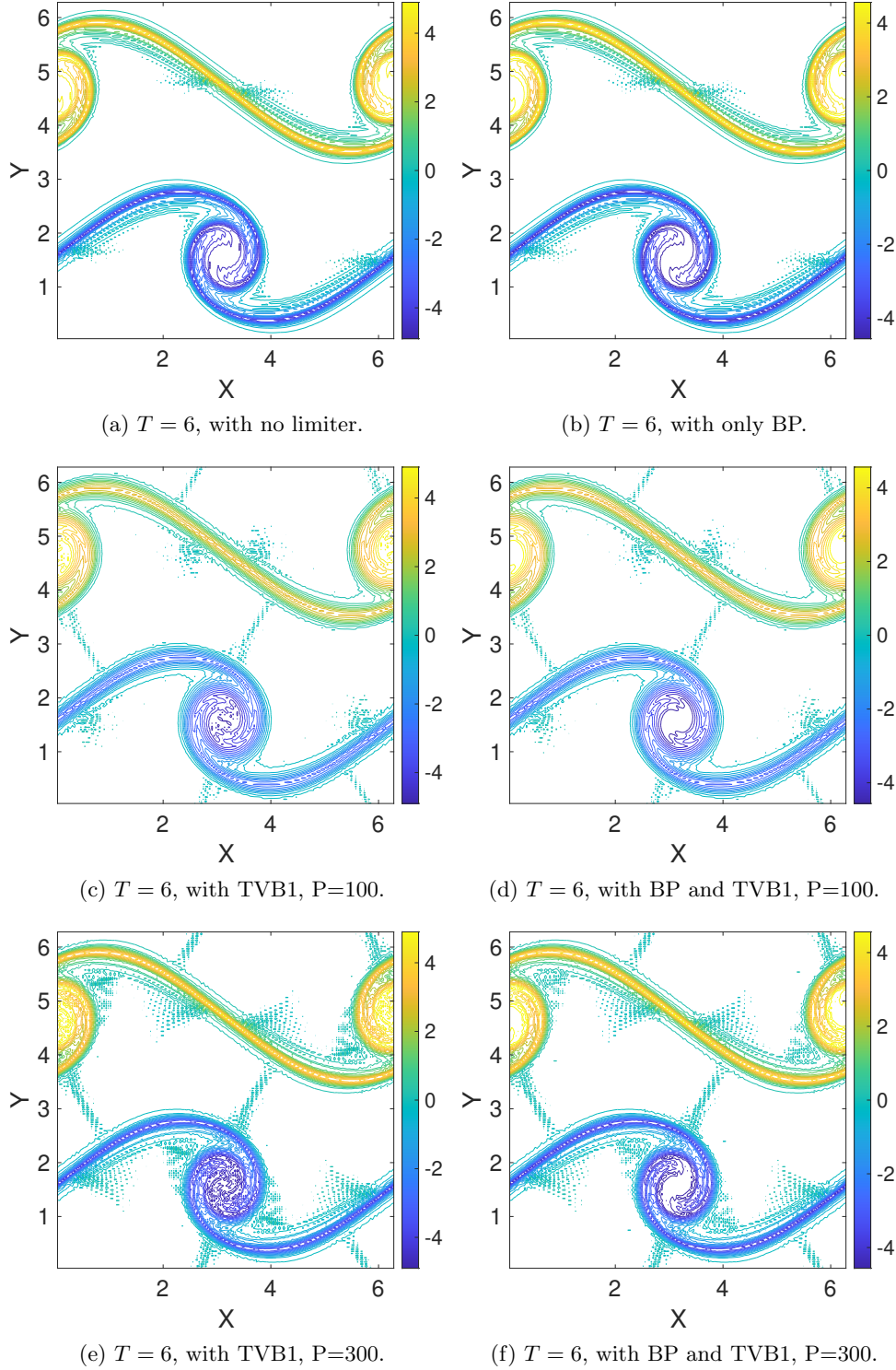


Fig. 1: Double shear layer problem. Fourth-order compact finite difference with SSP Runge–Kutta method on a 160×160 mesh solving the incompressible Euler equation (1.1) at $T = 6$. The time step is $\Delta t = \frac{1}{24 \max_x |u_0|} \Delta x$.

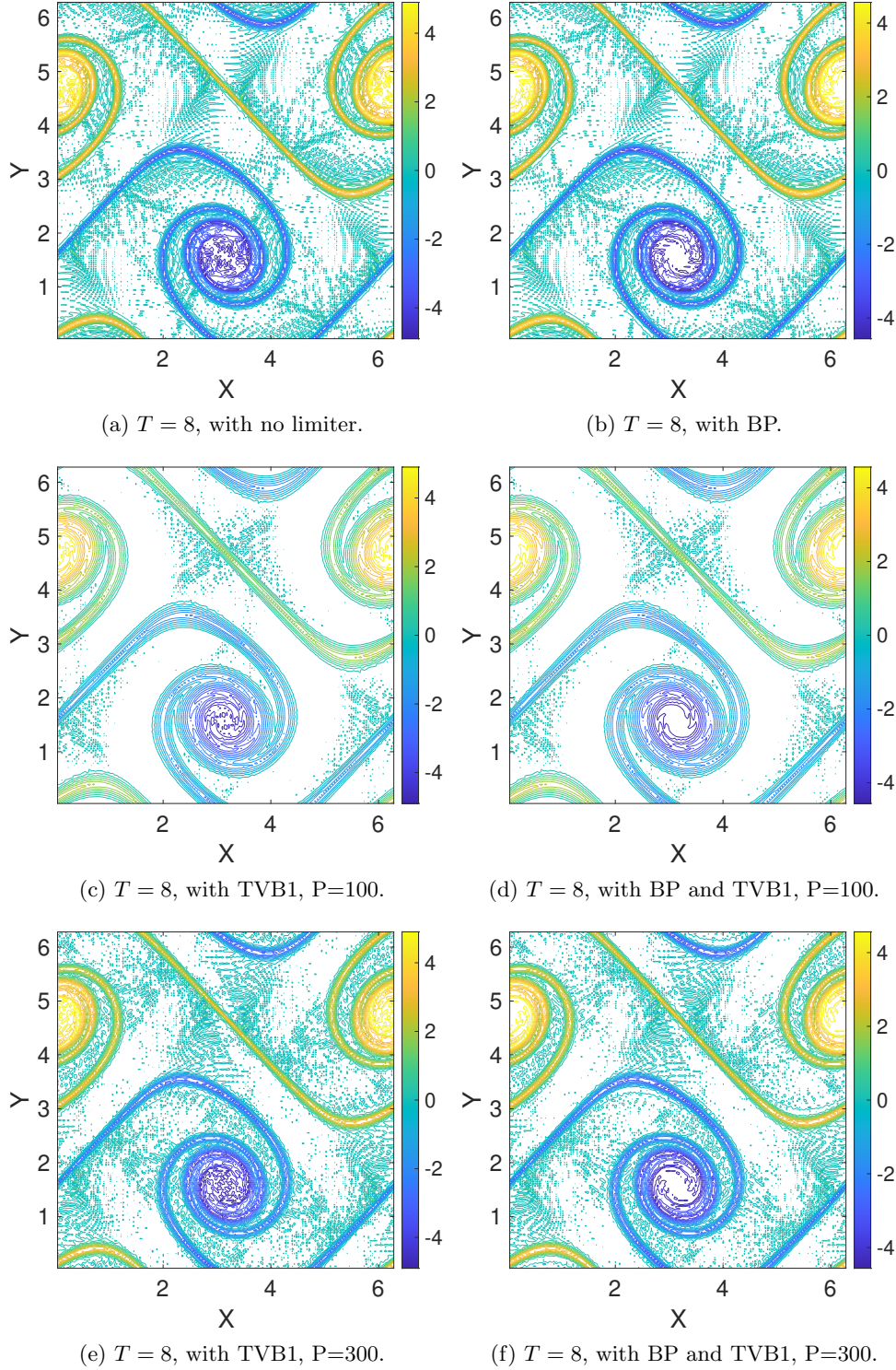


Fig. 2: Double shear layer problem. Fourth-order compact finite difference with SSP Runge–Kutta method on a 160×160 mesh solving the incompressible Euler equation (1.1) at $T = 8$. The time step is $\Delta t = \frac{1}{24 \max_x |u_0|} \Delta x$.

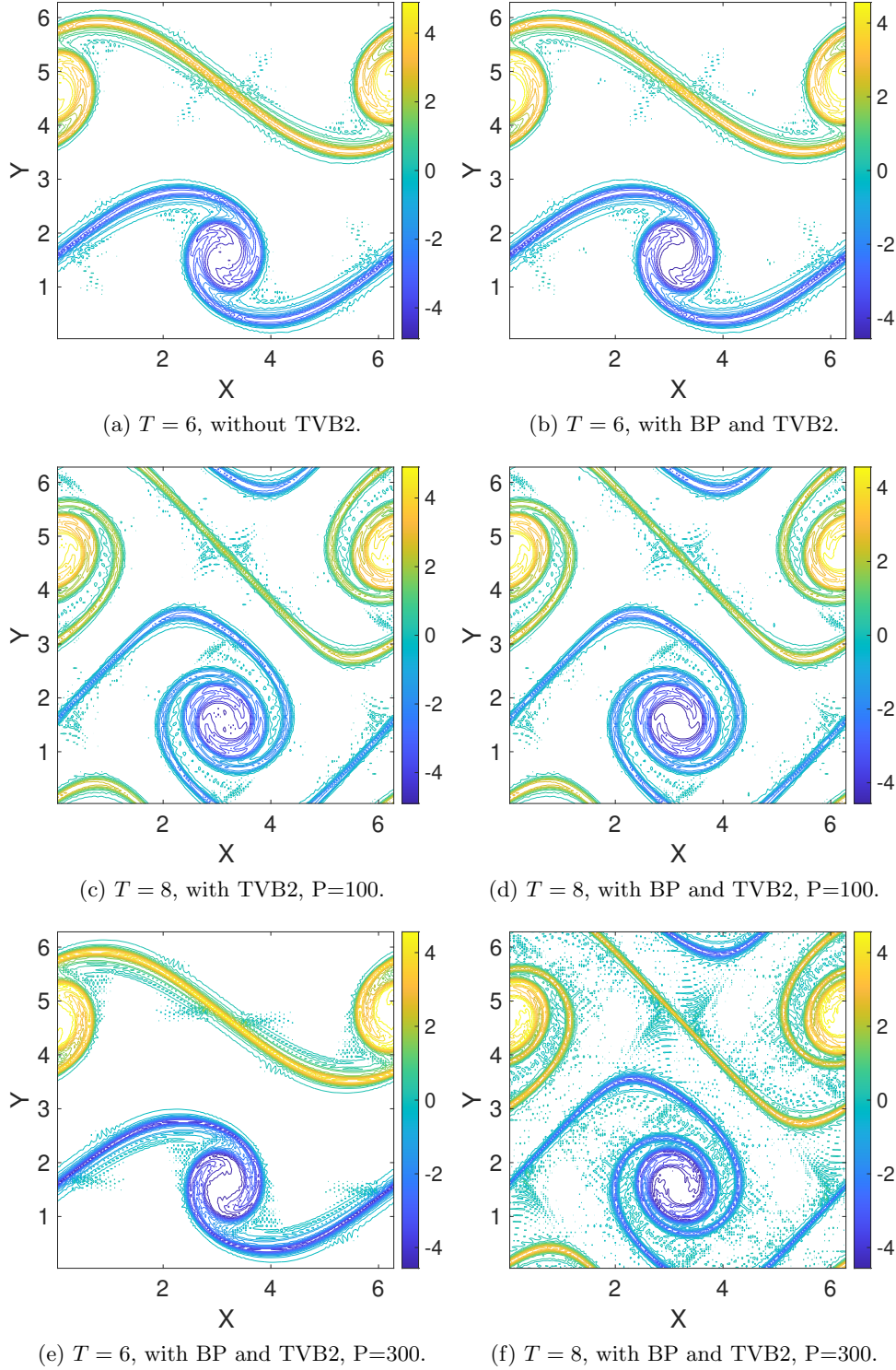


Fig. 3: Double shear layer problem. Fourth-order compact finite difference with SSP Runge–Kutta method on a 160×160 mesh solving the incompressible Euler equation (1.1) at $T = 6$ and $T = 8$. The time step is $\Delta t = \frac{1}{24 \max_x |\mathbf{u}_0|} \Delta x$.

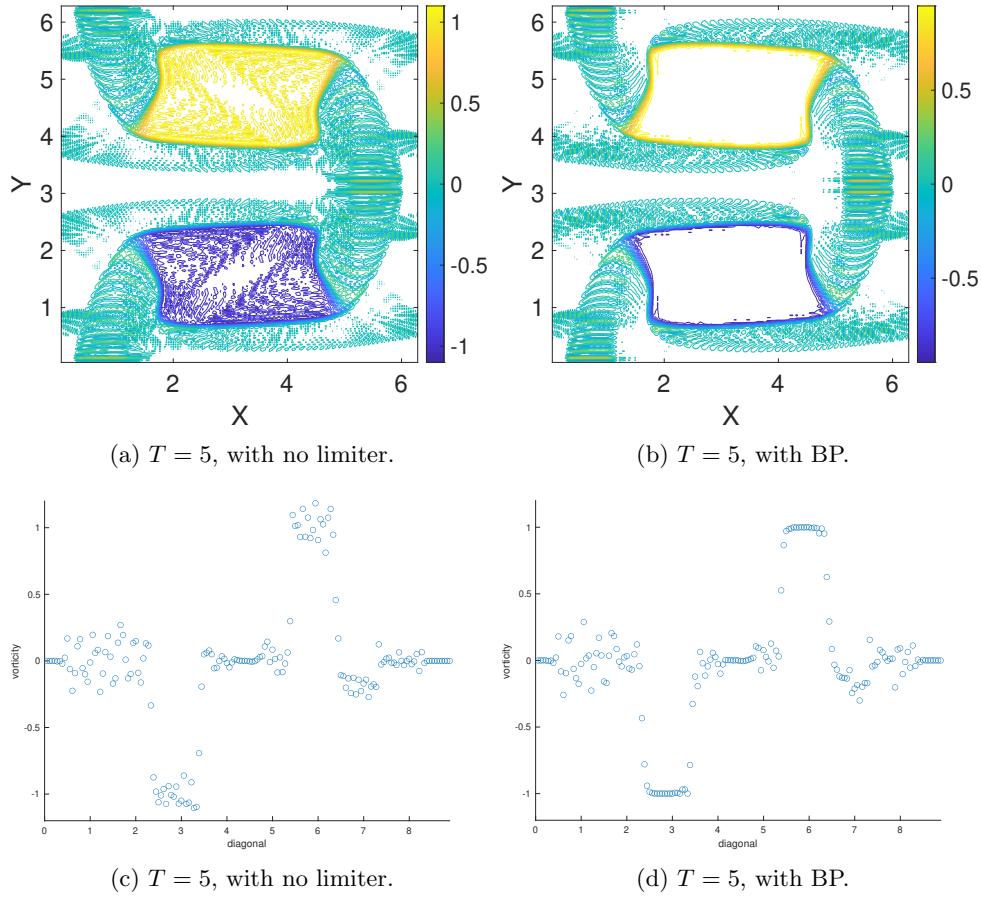


Fig. 4: A fourth-order accurate compact finite difference scheme for the incompressible Euler equation at $T = 5$ on a 160×160 mesh. The time step is $\Delta t = \frac{1}{24 \max |\mathbf{u}_0|} \Delta x$. The second row is the cut along the diagonal of the two-dimensional array.

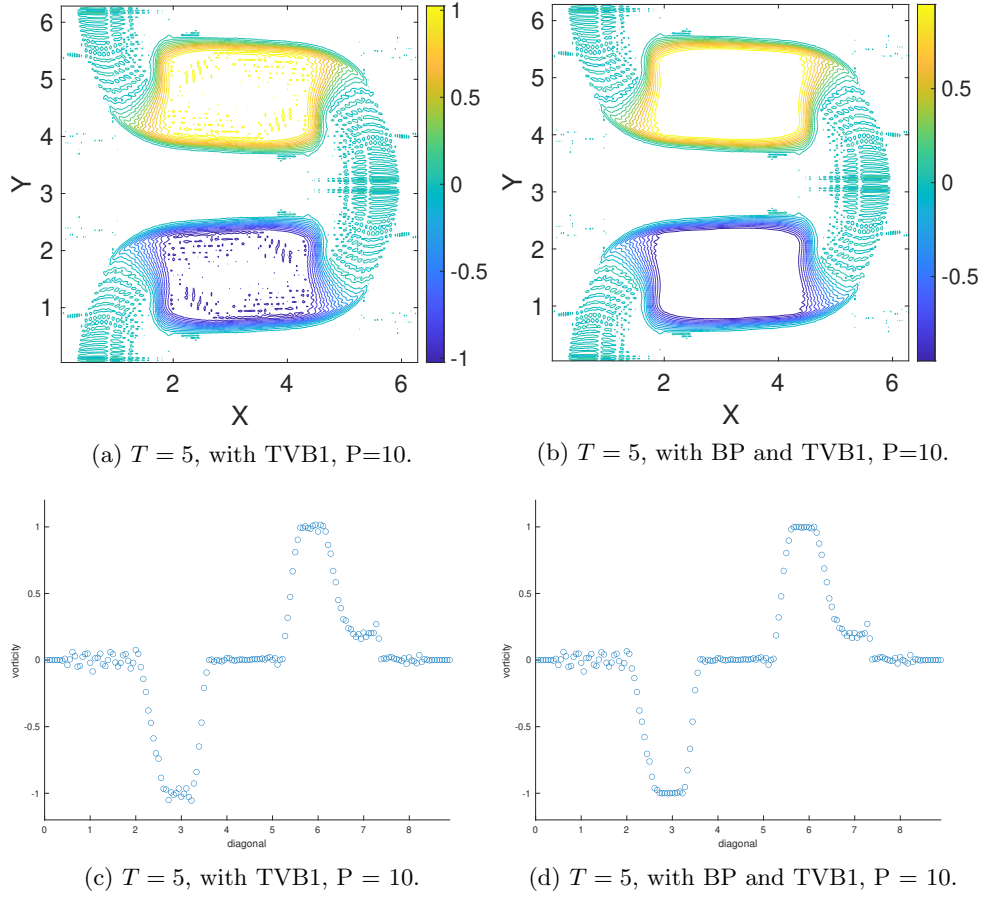


Fig. 5: A fourth-order accurate compact finite difference scheme for the incompressible Euler equation at $T = 5$ on a 160×160 mesh. The time step is $\Delta t = \frac{1}{24 \max |\mathbf{u}_0|} \Delta x$. The second row is the cut along the diagonal of the two-dimensional array.

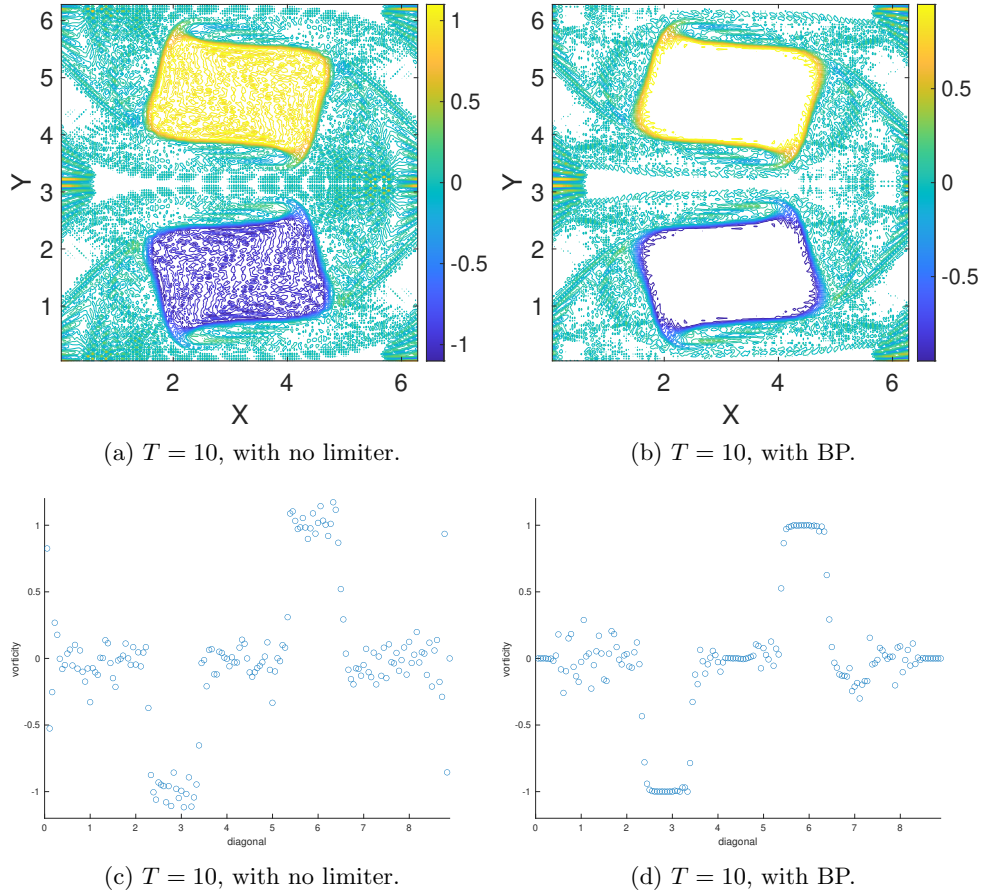


Fig. 6: A fourth-order accurate compact finite difference scheme for the incompressible Euler equation at $T = 5$ on a 160×160 mesh. The time step is $\Delta t = \frac{1}{24 \max |\mathbf{u}_0|} \Delta x$. The second row is the cut along the diagonal of the two-dimensional array.

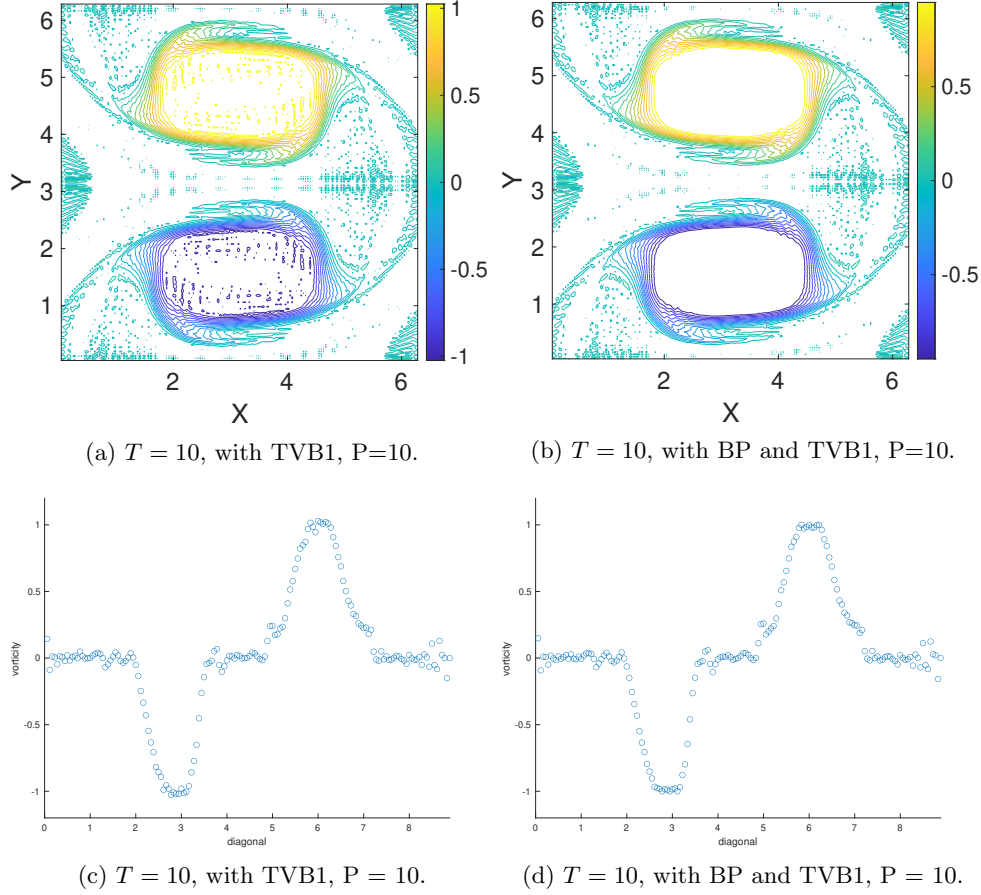


Fig. 7: A fourth-order accurate compact finite difference scheme for the incompressible Euler equation at $T = 10$ on a 160×160 mesh. The time step is $\Delta t = \frac{1}{12 \max |\mathbf{u}_0|} \Delta x$. The second row is the cut along the diagonal of the two-dimensional array.

341 **Appendix A: Comparison With The Nine-point Discrete Laplacian.**

342 Consider solving the two-dimensional Poisson equations $u_{xx} + u_{yy} = f$ with either
 343 homogeneous Dirichlet boundary conditions or periodic boundary conditions on a
 344 rectangular domain. Let \mathbf{u} be a $N_x \times N_y$ matrix with entries $u_{i,j}$ denoting the numerical
 345 solutions at a uniform grid $(x_i, y_j) = (\frac{i}{N_x}, \frac{j}{N_y})$. Let \mathbf{f} be a $N_x \times N_y$ matrix with
 346 entries $f_{i,j} = f(x_i, y_j)$. The fourth order compact finite difference method in Section
 347 2 for $u_{xx} + u_{yy} = f$ can be written as:

$$348 \quad (6.1) \quad \frac{1}{\Delta x^2} W_{2x}^{-1} D_{xx} \mathbf{u} + \frac{1}{\Delta y^2} W_{2y}^{-1} D_{yy} \mathbf{u} = f(\mathbf{u}).$$

349 For convenience, we introduce two matrices,

$$350 \quad U = \begin{pmatrix} u_{i-1,j+1} & u_{i,j+1} & u_{i+1,j+1} \\ u_{i-1,j} & u_{i,j} & u_{i+1,j} \\ u_{i-1,j-1} & u_{i,j-1} & u_{i+1,j-1} \end{pmatrix}, \quad F = \begin{pmatrix} f_{i-1,j+1} & f_{i,j+1} & f_{i+1,j+1} \\ f_{i-1,j} & f_{i,j} & f_{i+1,j} \\ f_{i-1,j-1} & f_{i,j-1} & f_{i+1,j-1} \end{pmatrix}.$$

351 Notice that the scheme (6.1) is equivalent to

$$352 \quad \frac{1}{\Delta x^2} W_{2y} D_{xx} \mathbf{u} + \frac{1}{\Delta y^2} W_{2x} D_{yy} \mathbf{u} = W_{2x} W_{2y} f(\mathbf{u}),$$

353 which can be written as

$$354 \quad (6.2) \quad \frac{1}{12\Delta x^2} \begin{pmatrix} 1 & -2 & 1 \\ 10 & -20 & 10 \\ 1 & -2 & 1 \end{pmatrix} : U + \frac{1}{12\Delta y^2} \begin{pmatrix} 1 & 10 & 1 \\ -2 & -20 & -2 \\ 1 & 10 & 1 \end{pmatrix} : U = \frac{1}{144} \begin{pmatrix} 1 & 10 & 1 \\ 10 & 100 & 10 \\ 1 & 10 & 1 \end{pmatrix} : F,$$

355 where $:$ denotes the sum of all entrywise products in two matrices of the same size.

356 In particular, if $\Delta x = \Delta y = h$, the scheme above reduces to

$$357 \quad \frac{1}{6h^2} \begin{pmatrix} 1 & 4 & 1 \\ 4 & -20 & 4 \\ 1 & 4 & 1 \end{pmatrix} : U = \frac{1}{144} \begin{pmatrix} 1 & 10 & 1 \\ 10 & 100 & 10 \\ 1 & 10 & 1 \end{pmatrix} : F.$$

358 Recall that the classical nine-point discrete Laplacian [4] for the Poisson equation can
 359 be written as

$$360 \quad (6.3) \quad \frac{1}{12\Delta x^2} \begin{pmatrix} 1 & -2 & 1 \\ 10 & -20 & 10 \\ 1 & -2 & 1 \end{pmatrix} : U + \frac{1}{12\Delta y^2} \begin{pmatrix} 1 & 10 & 1 \\ -2 & -20 & -2 \\ 1 & 10 & 1 \end{pmatrix} : U = \frac{1}{12} \begin{pmatrix} 0 & 1 & 0 \\ 1 & 8 & 1 \\ 0 & 1 & 0 \end{pmatrix} : F,$$

361 which reduces to the following under the assumption $\Delta x = \Delta y = h$,

$$362 \quad \frac{1}{6h^2} \begin{pmatrix} 1 & 4 & 1 \\ 4 & -20 & 4 \\ 1 & 4 & 1 \end{pmatrix} : U = \frac{1}{12} \begin{pmatrix} 0 & 1 & 0 \\ 1 & 8 & 1 \\ 0 & 1 & 0 \end{pmatrix} : F.$$

363 Both schemes (6.2) and (6.3) are fourth order accurate and they have the same stencil
 364 in the left hand side. As to which scheme produces smaller errors, it seems to be
 365 problem dependent, see Figure 8. Figure 8 shows the errors of two schemes (6.2) and
 366 (6.3) using uniform grids with $\Delta x = \frac{2}{3}\Delta y$ for solving the Poisson equation $u_{xx} + u_{yy} =$
 367 f on a rectangle $[0, 1] \times [0, 2]$ with Dirichlet boundary conditions. For solution 1, we
 368 have $u(x, y) = \sin(\pi x) \sin(\pi y) + 2x$, for solution 2, we have $u(x, y) = \sin(\pi x) \sin(\pi y) +$
 369 $4x^4 y^4$.

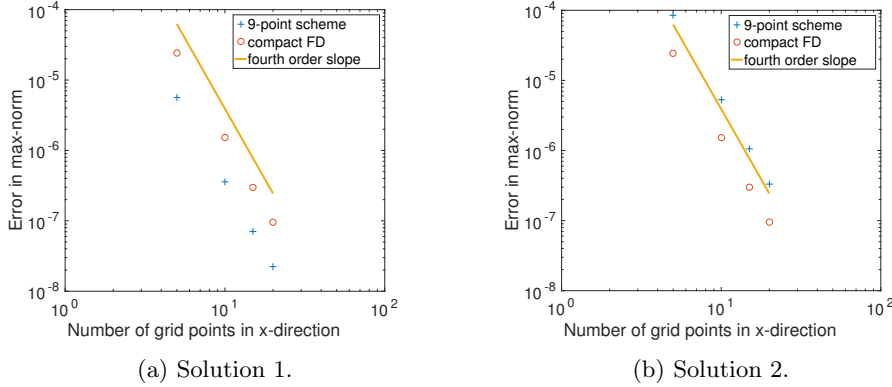


Fig. 8: Error comparison.

370 **Appendix B: M -matrices And A Discrete Maximum Principle.** Consider
 371 solving the heat equation $u_t = u_{xx} + u_{yy}$ with a periodic boundary condition. It is
 372 well known that a discrete maximum principle is satisfied under certain time step
 373 constraints if the spatial discretization is the nine-point discrete Laplacian or the
 374 compact scheme (6.1) with backward Euler and Crank-Nicolson time discretizations.
 375 For simplicity, we only consider the compact scheme (6.1) and the discussion for the
 376 nine-point discrete Laplacian is similar. Assume $\Delta x = \Delta y = h$. For backward Euler,
 377 the scheme can be written as

$$378 \quad \frac{1}{144} \begin{pmatrix} 1 & 10 & 1 \\ 10 & 100 & 10 \\ 1 & 10 & 1 \end{pmatrix} : (U^{n+1} - U^n) = \frac{\Delta t}{6h^2} \begin{pmatrix} 1 & 4 & 1 \\ 4 & -20 & 4 \\ 1 & 4 & 1 \end{pmatrix} : U^{n+1},$$

379 thus

$$380 \quad \frac{1}{144} \begin{pmatrix} 1 & 10 & 1 \\ 10 & 100 & 10 \\ 1 & 10 & 1 \end{pmatrix} : U^{n+1} - \frac{\Delta t}{6h^2} \begin{pmatrix} 1 & 4 & 1 \\ 4 & -20 & 4 \\ 1 & 4 & 1 \end{pmatrix} : U^{n+1} = \frac{1}{144} \begin{pmatrix} 1 & 10 & 1 \\ 10 & 100 & 10 \\ 1 & 10 & 1 \end{pmatrix} : U^n.$$

381 Let A and B denote the matrices corresponding to the operator in the left hand side
 382 and right hand side above respectively, then the scheme can be written as

$$383 \quad A\mathbf{u}^{n+1} = B\mathbf{u}^n,$$

384 and A is a M -Matrix (diagonally dominant, positive diagonal entries and non-positive
 385 off diagonal entries) under the following constraint which allows very large time steps:

$$386 \quad \frac{\Delta t}{h^2} \geq \frac{5}{48}.$$

387 The inverses of M -Matrices have non-negative entries, e.g., see [6]. Thus A^{-1} has
 388 non-negative entries. Moreover, it is straightforward to check that $A\mathbf{e} = \mathbf{e}$ where
 389 $\mathbf{e} = (1 \ 1 \ \dots \ 1)^T$. Thus $A^{-1}\mathbf{e} = \mathbf{e}$, which implies the sum of each row of A^{-1} is
 390 1 thus each row of A^{-1} multiplying any vector V is a convex combination of entries

391 of V . It is also obvious that each entry of B is non-negative and the sum of each row
 392 of B is 1. Therefore, $\mathbf{u}^{n+1} = A^{-1}B\mathbf{u}^n$ satisfies a discrete maximum principle:

$$393 \quad \min_{i,j} u_{i,j}^n \leq u_{i,j}^{n+1} \leq \max_{i,j} u_{i,j}^n.$$

394 For the second order accurate Crank-Nicolson time discretization, the scheme can
 395 be written as

$$396 \quad \frac{1}{144} \begin{pmatrix} 1 & 10 & 1 \\ 10 & 100 & 10 \\ 1 & 10 & 1 \end{pmatrix} : (U^{n+1} - U^n) = \frac{\Delta t}{6h^2} \begin{pmatrix} 1 & 4 & 1 \\ 4 & -20 & 4 \\ 1 & 4 & 1 \end{pmatrix} : \frac{U^{n+1} + U^n}{2},$$

397 thus

$$398 \quad \left[\frac{1}{144} \begin{pmatrix} 1 & 10 & 1 \\ 10 & 100 & 10 \\ 1 & 10 & 1 \end{pmatrix} - \frac{\Delta t}{12h^2} \begin{pmatrix} 1 & 4 & 1 \\ 4 & -20 & 4 \\ 1 & 4 & 1 \end{pmatrix} \right] : U^{n+1} =$$

$$399$$

$$400 \quad \left[\frac{1}{144} \begin{pmatrix} 1 & 10 & 1 \\ 10 & 100 & 10 \\ 1 & 10 & 1 \end{pmatrix} + \frac{\Delta t}{12h^2} \begin{pmatrix} 1 & 4 & 1 \\ 4 & -20 & 4 \\ 1 & 4 & 1 \end{pmatrix} \right] : U^n.$$

401 Let the matrix-vector form of the scheme above be $A\mathbf{u}^{n+1} = B\mathbf{u}^n$. Then for A to be
 402 an M -Matrix, we only need $\frac{\Delta t}{h^2} \geq \frac{5}{24}$. However, for B to have non-negative entries,
 403 we need $\frac{\Delta t}{h^2} \leq \frac{5}{12}$. Thus the Crank-Nicolson method can ensure a discrete maximum
 404 principle if the time step satisfies,

$$405 \quad \frac{5}{24}h^2 \leq \Delta t \leq \frac{5}{12}h^2.$$

406 Appendix C: Fast Poisson Solvers.

407 **Dirichlet boundary conditions.** Consider solving the Poisson equation $u_{xx} +$
 408 $u_{yy} = f(x, y)$ on a rectangular domain $[0, L_x] \times [0, L_y]$ with homogeneous Dirichlet
 409 boundary conditions. Assume we use the grid $x_i = i\Delta x$, $i = 0, \dots, N_x + 1$ with
 410 uniform spacing $\Delta x = \frac{L_x}{N_x + 1}$ for the x -variable and $y_j = j\Delta y$, $j = 0, \dots, N_y + 1$
 411 with uniform spacing $\Delta y = \frac{L_y}{N_y + 1}$ for y -variable. Let \mathbf{u} be a $N_x \times N_y$ matrix such
 412 that its (i, j) entry $u_{i,j}$ is the numerical solution at interior grid points (x_i, y_j) . Let
 413 \mathbf{F} be a $(N_x + 2) \times (N_y + 2)$ matrix with entries $f(x_i, y_j)$ for $i = 0, \dots, N_x + 1$ and
 414 $j = 0, \dots, N_y + 1$.

415 To obtain the matrix representation of the operator in (6.2) and (6.3), we consider
 416 two operators:

- 417 • Kronecker product of two matrices: if A is $m \times n$ and B is $p \times q$, then $A \otimes B$
 418 is $mp \times nq$ give by

$$419 \quad A \otimes B = \begin{pmatrix} a_{11}B & \cdots & a_{1n}B \\ \vdots & \vdots & \vdots \\ a_{m1}B & \cdots & a_{mn}B \end{pmatrix}.$$

- 420 • For a $m \times n$ matrix X , $\text{vec}(X)$ denotes a column vector of size mn made of
 421 the columns of X stacked atop one another from left to right.

422 The following properties will be used:

- 423 1. $(A \otimes B)(C \otimes D) = AC \otimes BD$.

424 2. $(A \otimes B)^{-1} = A^{-1} \otimes B^{-1}$.

425 3. $(B^T \otimes A) \text{vec}(X) = \text{vec}(AXB)$.

426 We define two tridiagonal square matrices of size $N_x \times N_x$:

427
$$D_{xx} = \begin{pmatrix} -2 & 1 & & & & & \\ 1 & -2 & 1 & & & & \\ & 1 & -2 & 1 & & & \\ & & \ddots & \ddots & \ddots & & \\ & & & 1 & -2 & 1 & \\ & & & & 1 & -2 & \end{pmatrix}, W_{2x} = \frac{1}{12} \begin{pmatrix} 10 & 1 & & & & & \\ 1 & 10 & 1 & & & & \\ & 1 & 10 & 1 & & & \\ & & \ddots & \ddots & \ddots & & \\ & & & 1 & 10 & 1 & \\ & & & & 1 & 10 & \end{pmatrix}.$$

428 Let \overline{W}_{2x} denote a $N_x \times (N_x + 2)$ tridiagonal matrix of the following form:

429 (6.4)
$$\overline{W}_{2x} = \frac{1}{12} \begin{pmatrix} 1 & 10 & 1 & & & & \\ & 1 & 10 & 1 & & & \\ & & \ddots & \ddots & \ddots & & \\ & & & 1 & 10 & 1 & \end{pmatrix}.$$

430 The matrices D_{yy} , W_{2y} and \overline{W}_{2y} are similarly defined.

431 Then the scheme (6.2) can be written in a matrix-vector form:

432
$$\frac{1}{\Delta x^2} D_{xx} \mathbf{u} W_{2y}^T + \frac{1}{\Delta y^2} W_{2x} \mathbf{u} D_{yy}^T = \overline{W}_{2x} \mathbf{F} \overline{W}_{2y}^T,$$

433 or equivalently,

434 (6.5)
$$\left(W_{2y} \otimes \frac{1}{\Delta x^2} D_{xx} + \frac{1}{\Delta y^2} D_{yy} \otimes W_{2x} \right) \text{vec}(\mathbf{u}) = (\overline{W}_{2x} \otimes \overline{W}_{2y}) \text{vec}(\mathbf{F}).$$

Let $\mathbf{h}_x = [h_1, h_2, \dots, h_{N_x}]^T$ with $h_i = \frac{i}{N_x+1}$, and $\sin(m\pi\mathbf{h}_x)$ denote a column vector of size N_x with its i -th entry being $\sin(m\pi h_i)$. Then $\sin(m\pi\mathbf{h}_x)$ are the eigenvectors of D_{xx} and W_{2x} with the associated eigenvalues being $2 \cos(\frac{m\pi}{N_x+1}) - 2$ and $\frac{5}{6} + \frac{1}{6} \cos(\frac{m\pi}{N_x+1})$ respectively for $m = 1, \dots, N_x$. Let

$$S_x = [\sin(\pi\mathbf{h}_x), \sin(2\pi\mathbf{h}_x), \dots, \sin(N_x\pi\mathbf{h}_x)]$$

435 be the $N_x \times N_x$ eigenvector matrix, then S_x is a symmetric matrix. Let Λ_{1x} denote
436 a diagonal matrix with diagonal entries $2 \cos(\frac{m\pi}{N_x+1}) - 2$ and Λ_{2x} denote a diagonal
437 matrix with diagonal entries $\frac{5}{6} + \frac{1}{6} \cos(\frac{m\pi}{N_x+1})$, then we have $D_{xx} = S_x \Lambda_{1x} S_x^{-1}$ and
438 $W_{2x} = S_x \Lambda_{2x} S_x^{-1}$, thus

439
$$W_{2y} \otimes D_{xx} = (S_y \Lambda_{2y} S_y^{-1}) \otimes (S_x \Lambda_{1x} S_x^{-1}) = (S_y \otimes S_x) (\Lambda_{2y} \otimes \Lambda_{1x}) (S_y^{-1} \otimes S_x^{-1}).$$

440 The scheme can be written as

441
$$(S_y \otimes S_x) \left(\frac{1}{\Delta x^2} \Lambda_{2y} \otimes \Lambda_{1x} + \frac{1}{\Delta y^2} \Lambda_{1y} \otimes \Lambda_{2x} \right) (S_y^{-1} \otimes S_x^{-1}) \text{vec}(\mathbf{u}) = (\overline{W}_{2y} \otimes \overline{W}_{2x}) \text{vec}(\mathbf{F}).$$

442 Let Λ be a $N_x \times N_y$ matrix with $\Lambda_{i,j}$ being equal to

443
$$\frac{1}{3\Delta x^2} \left(\cos\left(\frac{i\pi}{N_x+1}\right) - 1 \right) \left(\cos\left(\frac{m\pi}{N_y+1}\right) + 5 \right) + \frac{1}{3\Delta y^2} \left(\cos\left(\frac{m\pi}{N_x+1}\right) + 5 \right) \left(\cos\left(\frac{j\pi}{N_y+1}\right) - 1 \right),$$

444 then $\text{vec}(\Lambda)$ are precisely the diagonal entries of the diagonal matrix $\frac{1}{\Delta x^2} \Lambda_{2y} \otimes \Lambda_{1x} +$
 445 $\frac{1}{\Delta y^2} \Lambda_{1y} \otimes \Lambda_{2x}$, then the scheme above is equivalent to

$$446 \quad S_x(\Lambda \circ (S_x^{-1} \mathbf{u} S_y^{-1})) S_y = \overline{W}_{2x} \mathbf{F} \overline{W}_{2y}^T,$$

447 where the symmetry of S matrices is used. The solution is given by

$$448 \quad (6.6) \quad \mathbf{u} = S_x \{ [S_x^{-1} (\overline{W}_{2x} \mathbf{F} \overline{W}_{2y}^T) S_y^{-1}] ./ \Lambda \} S_y,$$

449 where $./$ denotes the entrywise division for two matrices of the same size.

450 Since the multiplication of the matrices S and S^{-1} can be implemented by the
 451 *Discrete Sine Transform*, (6.6) gives a fast Poisson solver.

452 For nonhomogeneous Dirichlet boundary conditions, the fourth order accurate
 453 compact finite difference scheme can also be written in the form of (6.5):

$$454 \quad (6.7) \quad \left(W_{2y} \otimes \frac{1}{\Delta x^2} D_{xx} + \frac{1}{\Delta y^2} D_{yy} \otimes W_{2x} \right) \text{vec}(\mathbf{u}) = \text{vec}(\tilde{\mathbf{F}}),$$

455 where $\tilde{\mathbf{F}}$ consists of both \mathbf{F} and the Dirichlet boundary conditions. Thus the scheme
 456 can still be efficiently implemented by the *Discrete Sine Transform*.

457 **Periodic boundary conditions.** For periodic boundary conditions on a rect-
 458 angular domain, we should consider the uniform grid $x_i = i\Delta x$, $i = 1, \dots, N_x$ with
 459 $\Delta x = \frac{L_x}{N_x}$ and $y_j = j\Delta y$, $j = 1, \dots, N_y$ with uniform spacing $\Delta y = \frac{L_y}{N_y}$, then the
 460 fourth order accurate compact finite difference scheme can still be written in the
 461 form of (6.5) with the D_{xx} , D_{yy} , W_{2x} and W_{2y} matrices being redefined as circulant
 462 matrices:

$$463 \quad D_{xx} = \begin{pmatrix} -2 & 1 & & & 1 \\ 1 & -2 & 1 & & \\ & 1 & -2 & 1 & \\ & & \ddots & \ddots & \ddots \\ & & & 1 & -2 & 1 \\ 1 & & & & 1 & -2 \end{pmatrix}, W_{2x} = \frac{1}{12} \begin{pmatrix} 10 & 1 & & & 1 \\ 1 & 10 & 1 & & \\ & 1 & 10 & 1 & \\ & & \ddots & \ddots & \ddots \\ & & & 1 & 10 & 1 \\ 1 & & & & 1 & 10 \end{pmatrix}.$$

464 The Discrete Fourier Matrix is the eigenvector matrix for any circulant matrices,
 465 and the corresponding eigenvalues are for D_{xx} and W_{2x} are $2 \cos(\frac{m2\pi}{N_x}) - 2$ and
 466 $\frac{1}{6} \cos(\frac{m2\pi}{N_x}) + \frac{5}{6}$ for $m = 0, 1, 2, \dots, N_x - 1$. The matrix $W_{2y} \otimes \frac{1}{\Delta x^2} D_{xx} + \frac{1}{\Delta y^2} D_{yy} \otimes W_{2x}$
 467 is singular because its first eigenvalue $\Lambda_{1,1}$ is zero. Nonetheless, the scheme can still be
 468 implemented by solving (6.6) with Fast Fourier Transform. For the zero eigenvalue,
 469 we can simply reset the division by eigenvalue zero to zero. Since the eigenvector
 470 for eigenvalue zero is $\mathbf{e} = (1 \ 1 \ \dots \ 1)^T$, and the columns of the Discrete Fourier
 471 Matrix are orthogonal to one another, resetting the division by eigenvalue zero to zero
 472 simply means that we obtain a numerical solution satisfying $\sum_i \sum_j u_{i,j} = 0$. And
 473 this is also the least square solution to the singular linear system.

474 **Neumann boundary conditions.** For Dirichlet and periodic boundary condi-
 475 tions, we can invert the matrix coefficient matrix in (6.5) using eigenvectors of much
 476 smaller matrices W_{2x} and D_{xx} due to the fact that $W_{2x} - \frac{1}{12} D_{xx}$ is the identity matrix
 477 *Id*. Here we discuss how to achieve a fourth order accurate boundary approximation

478 for Neumann boundary conditions by keeping $W_{2x} - \frac{1}{12}D_{xx} = Id$. We first consider
 479 a one-dimensional problem with homogeneous Neumann boundary conditions:

$$480 \quad u''(x) = f(x), x \in [0, L_x],$$

$$481 \quad u'(0) = u'(L_x) = 0.$$

483 Assume we use the uniform grid $x_i = i\Delta x$, $i = 0, \dots, N_x + 1$ with $\Delta x = \frac{L_x}{N_x + 1}$. The
 484 two boundary point values u_0 and $u_{N_x + 1}$ can be expressed in terms of interior point
 485 values through boundary conditions. For approximating the boundary conditions, we
 486 can apply the fourth order one-sided difference at $x = 0$:

$$487 \quad u'(0) \approx \frac{-25u(0) + 48u(\Delta x) - 36u(2\Delta x) + 16u(3\Delta x) - 3u(4\Delta x)}{12\Delta x}$$

488 which implies the finite difference approximation:

$$489 \quad u_0 = \frac{48u_1 - 36u_2 + 16u_3 - 3u_4}{25}.$$

490 Define two column vectors:

$$491 \quad \mathbf{u} = [u_1, u_2, \dots, u_{N_x}]^T, \quad \mathbf{f} = [f(x_0), f(x_1), \dots, f(x_{N_x}), f(x_{N_x + 1})]^T,$$

492 then a fourth order accurate compact finite difference scheme can be written as

$$493 \quad \frac{1}{\Delta x^2} \bar{D}_{xx} I_x \mathbf{u} = \bar{W}_{2x} \mathbf{f},$$

494 where \bar{W}_{2x} is the same as in (6.4), and \bar{D}_{xx} is a matrix of size $N_x \times (N_x + 2)$ and I_x
 495 is a matrix of size $(N_x + 2) \times N_x$:

$$496 \quad \bar{D}_{xx} = \begin{pmatrix} 1 & -2 & 1 & & & & \\ & 1 & -2 & 1 & & & \\ & & \ddots & \ddots & \ddots & & \\ & & & & 1 & -2 & 1 \end{pmatrix}, \quad I_x = \begin{pmatrix} \frac{48}{25} & -\frac{36}{25} & \frac{16}{25} & -\frac{3}{25} & & & \\ & 1 & & & & & \\ & & 1 & & & & \\ & & & \ddots & & & \\ & & & & & & 1 \\ & & & & -\frac{3}{25} & \frac{16}{25} & -\frac{36}{25} & \frac{48}{25} \end{pmatrix}.$$

497 Now consider solving the Poisson equation $u_{xx} + u_{yy} = f(x, y)$ on a rectangular domain
 498 $[0, L_x] \times [0, L_y]$ with homogeneous Neumann boundary conditions. Assume we use the
 499 grid $x_i = i\Delta x$, $i = 0, \dots, N_x + 1$ with $\Delta x = \frac{L_x}{N_x + 1}$ and $y_j = j\Delta y$, $j = 0, \dots, N_y + 1$
 500 with uniform spacing $\Delta y = \frac{L_y}{N_y + 1}$. Let \mathbf{u} be a $N_x \times N_y$ matrix such that $u_{i,j}$ is
 501 the numerical solution at (x_i, y_j) and \mathbf{F} be a $(N_x + 2) \times (N_y + 2)$ matrix with entries
 502 $f(x_i, y_j)$ ($i = 0, \dots, N_x + 1, j = 0, \dots, N_y + 1$). Then a fourth order accurate compact
 503 finite difference scheme can be written as

$$504 \quad \frac{1}{\Delta x^2} \bar{D}_{xx} I_x \mathbf{u} I_y^T \bar{W}_{2y}^T + \frac{1}{\Delta y^2} \bar{W}_{2x} I_x \mathbf{u} I_y^T \bar{D}_{yy}^T = \bar{W}_{2x} \mathbf{F} \bar{W}_{2y}^T.$$

505 Let $D_{xx} = \bar{D}_{xx} I_x$ and $W_{2x} = \bar{W}_{2x} I_x$, then the scheme can be written as (6.5).

506 Notice that $W_{2x} - \frac{1}{12}D_{xx} = (\bar{W}_{2x} - \frac{1}{12}\bar{D}_{xx})I_x$ is still the identity matrix thus
 507 W_{2x} and D_{xx} still have the same eigenvectors. Let S be the eigenvector matrix
 508 and Λ_1 and Λ_2 be diagonal matrices with eigenvalues, then the scheme can still be

509 implemented as (6.6). The eigenvectors S and the eigenvalues can be obtained by
 510 computing eigenvalue problems for two small matrices D_{xx} of size $N_x \times N_x$ and D_{yy}
 511 of size $N_y \times N_y$. If such a Poisson problem needs to be solved in each time step
 512 in a time-dependent problem such as the incompressible flow equations, then this is
 513 an efficient Poisson solver because S and Λ can be computed before time evolution
 514 without considering eigenvalue problems for any matrix of size $N_x N_y \times N_x N_y$.

515 For nonhomogeneous Neumann boundary conditions, the point values of u along
 516 the boundary should be expressed in terms of interior ones as follows:

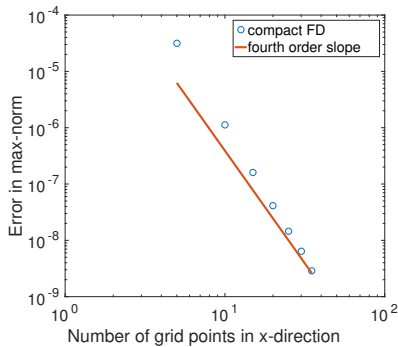
517 1. First obtain the point values except the two cell ends (i.e., corner points of
 518 the rectangular domain) for each of the four boundary line segments. For
 519 instance, if the left boundary condition is $\frac{\partial u}{\partial x}(0, y) = g(y)$, then we obtain

$$520 \quad u_{0,j} = \frac{48u_{1,j} - 36u_{2,j} + 16u_{3,j} - 3u_{4,j} + 12\Delta x g(y_j)}{25}, \quad j = 1, \dots, N_y.$$

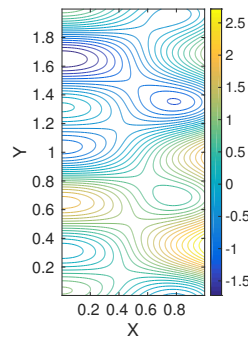
521 2. Second, obtain the approximation at four corners using the point values along
 522 the boundary. For instance, if the bottom boundary condition is $\frac{\partial u}{\partial y}(x, 0) =$
 523 $h(x)$, then

$$524 \quad u_{0,0} = \frac{48u_{1,0} - 36u_{2,0} + 16u_{3,0} - 3u_{4,0} + 12\Delta y h(0)}{25}$$

525 The scheme can still be written as (6.7) with $\tilde{\mathbf{F}}$ consisting of \mathbf{F} and the nonhomo-
 526 geneous boundary conditions. Notice that the matrix in (6.7) is singular thus we need to
 527 reset the division by eigenvalue zero to zero, which however no longer means that the
 528 obtained solution satisfies $\sum_i \sum_j u_{i,j} = 0$ since the eigenvectors are not necessarily or-
 529 thogonal to one another. See Figure 9 for the accuracy test of the fourth order compact
 530 finite difference scheme using uniform grids with $\Delta x = \frac{3}{2}\Delta y$ for solving the Poisson
 531 equation $u_{xx} + u_{yy} = f$ on a rectangle $[0, 1] \times [0, 2]$ with nonhomogeneous Neumann
 532 boundary conditions. The exact solution is $u(x, y) = \cos(\pi x) \cos(3\pi y) + \sin(\pi y) + x^4$.
 533 Since the solutions to Neumann boundary conditions are unique up to any constant,
 534 when computing errors, we need to add a constant $\frac{1}{N_x} \frac{1}{N_y} \sum_{i,j} [u(x_i, y_j) - u_{i,j}]$ to each
 535 entry of \mathbf{u} .



(a) Convergence rate.



(b) The contour of the solution.

Fig. 9: Accuracy test for Neumann boundary condition.

536 **Statements and Declarations.**

537 **Funding.** The research is supported by NSF DMS-1913120.

538 **Conflict of interest.** On behalf of all authors, the corresponding author states
539 that there is no conflict of interest.

540

REFERENCES

- 541 [1] B. COCKBURN AND C.-W. SHU, *TVB runge-kutta local projection discontinuous galerkin finite*
542 *element method for conservation laws. ii. general framework*, Mathematics of Computa-
543 tion, 52 (1989), pp. 411–435.
- 544 [2] B. COCKBURN AND C.-W. SHU, *Nonlinearly stable compact schemes for shock calculations*,
545 SIAM Journal on Numerical Analysis, 31 (1994), pp. 607–627.
- 546 [3] S. GOTTLIEB, D. I. KETCHESON, AND C.-W. SHU, *Strong stability preserving Runge-Kutta and*
547 *multistep time discretizations*, World Scientific, 2011.
- 548 [4] R. J. LEVEQUE, *Finite difference methods for ordinary and partial differential equations:*
549 *steady-state and time-dependent problems*, SIAM, 2007.
- 550 [5] H. LI, S. XIE, AND X. ZHANG, *A high order accurate bound-preserving compact finite difference*
551 *scheme for scalar convection diffusion equations*, SIAM Journal on Numerical Analysis,
552 56 (2018), pp. 3308–3345.
- 553 [6] T. QIN AND C.-W. SHU, *Implicit positivity-preserving high-order discontinuous galerkin meth-*
554 *ods for conservation laws*, SIAM Journal on Scientific Computing, 40 (2018), pp. A81–
555 A107.
- 556 [7] C.-W. SHU, *TVB uniformly high-order schemes for conservation laws*, Mathematics of Com-
557 putation, 49 (1987), pp. 105–121.
- 558 [8] X. ZHANG, Y. LIU, AND C.-W. SHU, *Maximum-principle-satisfying high order finite volume*
559 *weighted essentially nonoscillatory schemes for convection-diffusion equations*, SIAM Jour-
560 nal on Scientific Computing, 34 (2012), pp. A627–A658.
- 561 [9] X. ZHANG AND C.-W. SHU, *On maximum-principle-satisfying high order schemes for scalar*
562 *conservation laws*, Journal of Computational Physics, 229 (2010), pp. 3091–3120.
- 563 [10] Y. ZHANG, X. ZHANG, AND C.-W. SHU, *Maximum-principle-satisfying second order discontin-*
564 *uous Galerkin schemes for convection–diffusion equations on triangular meshes*, Journal
565 of Computational Physics, 234 (2013), pp. 295–316.